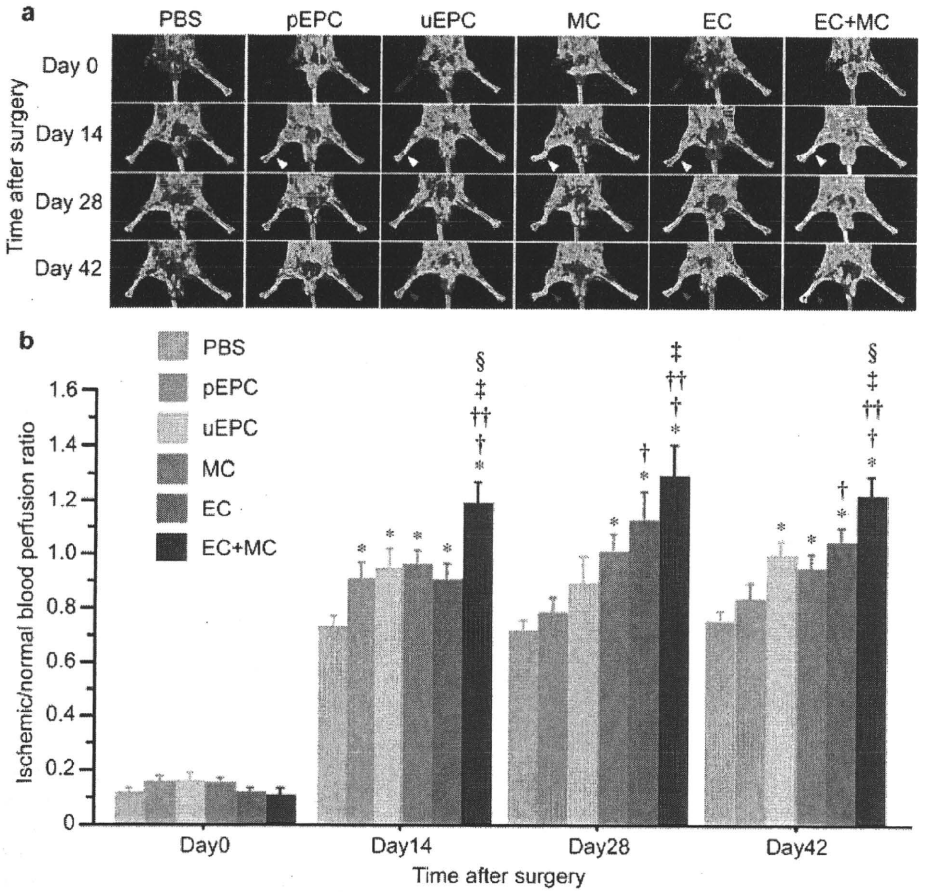

Figure 4. Augmented vascular regeneration by intra-arterial transplantation of human VPC-derived vascular cells in a murine hindlimb ischemia model. a) Serial LDPI analysis in hindlimb ischemia mice. At day 14, the blood flow of ischemic limbs in all cell transplanted groups increased significantly compared to the control group (white arrowhead). After 42 days, significant blood flow recovery was observed in the uEPC and human VPC-derived EC and/or MC-transplanted groups (red arrowhead), but not in pEPC. b) Quantitative analysis of hindlimb blood flow by calculating the ischemic/normal limb perfusion ratios after the induction of hindlimb ischemia. *$P<0.05$ vs. control, †$P<0.05$ vs. pEPC, ††$P<0.05$ vs. uEPC, ‡$P<0.05$ vs. MC, §$P<0.05$ vs. EC.
doi:10.1371/journal.pone.0001666.g004

stage successfully promoted vascular regeneration in the setting of tissue ischemia. After the expansion of human VPC-derived EC and MC, when intra-arterially administered, these cells significantly augmented neovascularization in an animal model of experimentally-induced hindlimb ischemia, compared to human peripheral blood and umbilical cord-derived EPC (pEPC and uEPC). Furthermore, the combined transplantation of human VPC-derived EC and MC could markedly induce vascular regeneration, compared to the single fraction transplantation of VPC-derived vascular cells (EC or MC). We also succeeded in demonstrating that transplanted human VPC-derived vascular cells were incorporated into the host circulation as both EC and MC. These results indicate that the combined transplantation of human VPC-derived EC and MC may have utility as a novel strategy for vascular regenerative medicine.

In the present study we used human VPC-derived VEGFR2$^+$ VE-cadherin$^+$ cells for the expansion and transplantation of EC. VEGFR2$^+$VE-cadherin$^+$ cells, obtained at day 10 of differentiation, were also positive for CD34 and therefore considered to be EC at the early differentiation stage (Figure 3) [9]. Even after 6 passages, 20~40% of these cells exhibited the expression of VEGFR2, VE-cadherin, and CD34, which indicated that they still retained the phenotype of EC at the early differentiated stage. Compared to EPC, transplantation of these EC significantly augmented ischemia-induced neovascularization. In contrast, we found that ischemia-induced neovascularization was not improved in mice receiving human aortic endothelial cells [4]. Therefore, human VPC-derived EC at the early differentiation stage might possess vascular regenerative capacity and these EC can be a valuable source for promoting vascular regeneration.

After expansion of human VPC-derived VEGFR2$^+$VE-cadherin$^+$ cells, about 70% of the expanded cells were αSMA positive. However, these cells were negative for the mature mural cell markers, including calponin, SM1, SM2, and h-caldesmon (data not shown). In contrast, expanded VEGFR2$^+$ VE-cadherin$^-$ cells obtained from human VPC under platelet derived growth factor (PDGF)-BB stimulation were positive for αSMA, calponin, SM1, and SM2, but negative for h-caldesmon. HAoSMC was positive for all of the mature MC markers, including h-caldesmon. In another series of our experiments, the mice receiving hAoSMC transplantation exhibited no significant improvement of neovascularization after the induction of ischemic hindlimbs (data not shown). Because h-caldesmon and calponin were reported to be expressed relatively late in SMC differentiation [10], human VPC-derived MC might be at a rather early "immature" differentiation

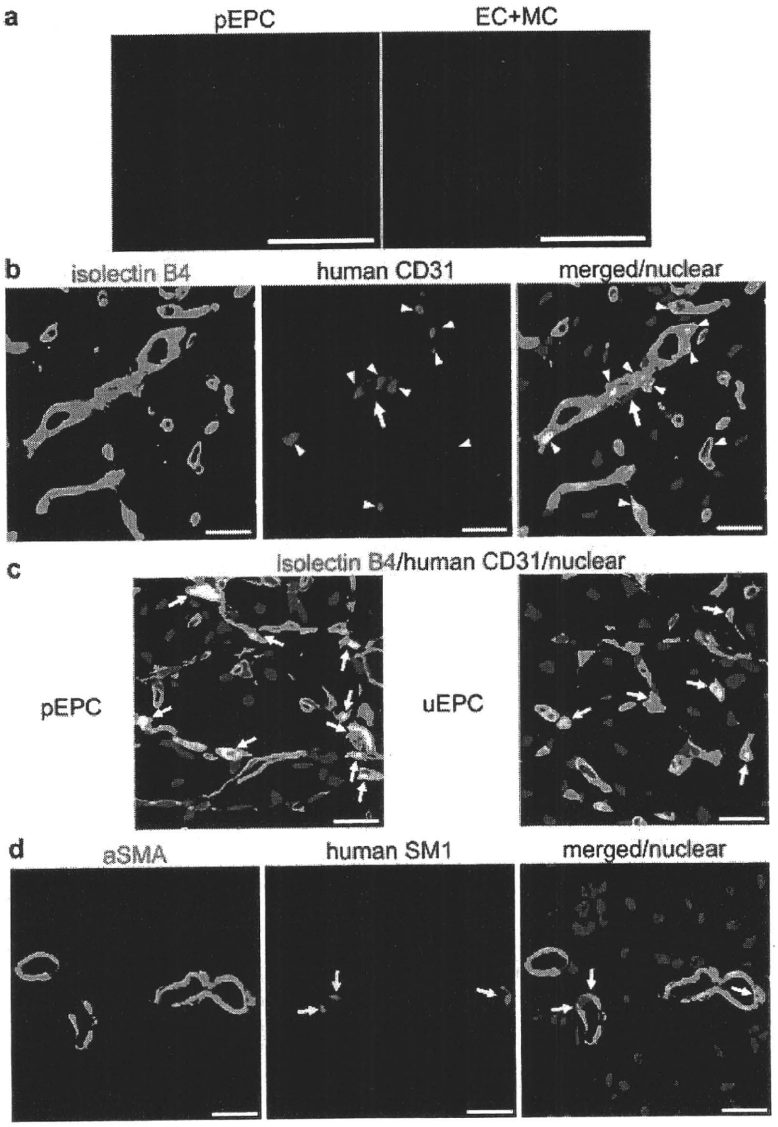

Figure 5. Incorporated human VPC-derived vascular cells at the sites of vascular regeneration. a) Transplanted CM-DiI (red) labeled pEPC or VPC-derived vascular cells in ischemic hindlimbs at day 7 were detected by the fluorescence stereomicroscope. Scale bar: 500 μm. b, c) Immunostaining of frozen sections harvested from ischemic limb tissues at day 14. Fluorescence staining of GSL I-isolectin B4 (green) and human CD31 (blue) with nuclear staining (red) in human VPC-derived EC+MC (b), pEPC, and uEPC (c) transplanted mice. Scale bar: 20 μm. d) Immunostaining of αSMA (green)/human SM1 (blue) with nuclear staining (red) in human VPC-derived EC+MC-transplanted mice at day 14. Scale bar: 20 μm.
doi:10.1371/journal.pone.0001666.g005

stage compared to hAoSMC, and thus, MC could be incorporated into the site of neovascularization.

Recently, Ferreira et al. reported that transplantation of human ES cells-derived EC into nude mice using Matrigel as scaffold contributed for the formation of blood vessels [11]. However, they did not show the direct integration of transplanted human ES cells-derived EC into host blood vessels. Judging from the double staining using intravenously injected isolectin B_4 and anti-human specific CD31 antibody, we found that the transplanted human VPC-derived EC incorporated into host circulating vessels. These transplanted EC could solely form de novo capillaries. In addition, by the double immunostaining of human SM1 and αSMA, we confirmed that transplanted human VPC-derived MC was also incorporated into host vessel walls. Therefore, transplanted human VPC-derived EC and MC structurally contributed to form new vessels in the process of vascular regeneration.

Interaction between EC and MC is essential for vascular development and maintenance of vascular stability [12,13]. Compared to only EC or MC-transplanted mice, the mice transplanted with the combined transplantation of EC and MC showed significant improvement after the induction of ischemic hindlimb. At day 42, the blood flow in the EC+MC group was significantly higher compared to only the EC or MC-transplanted groups. Not only mouse and/or human CD31 but also αSMA positive capillary density at day 42 significantly increased in the EC+MC group. We also found that the density of αSMA positive arterioles also significantly increased in the EC+MC group. These results indicated that combined transplantation of human VPC-derived EC and MC could synergistically contribute to vascular

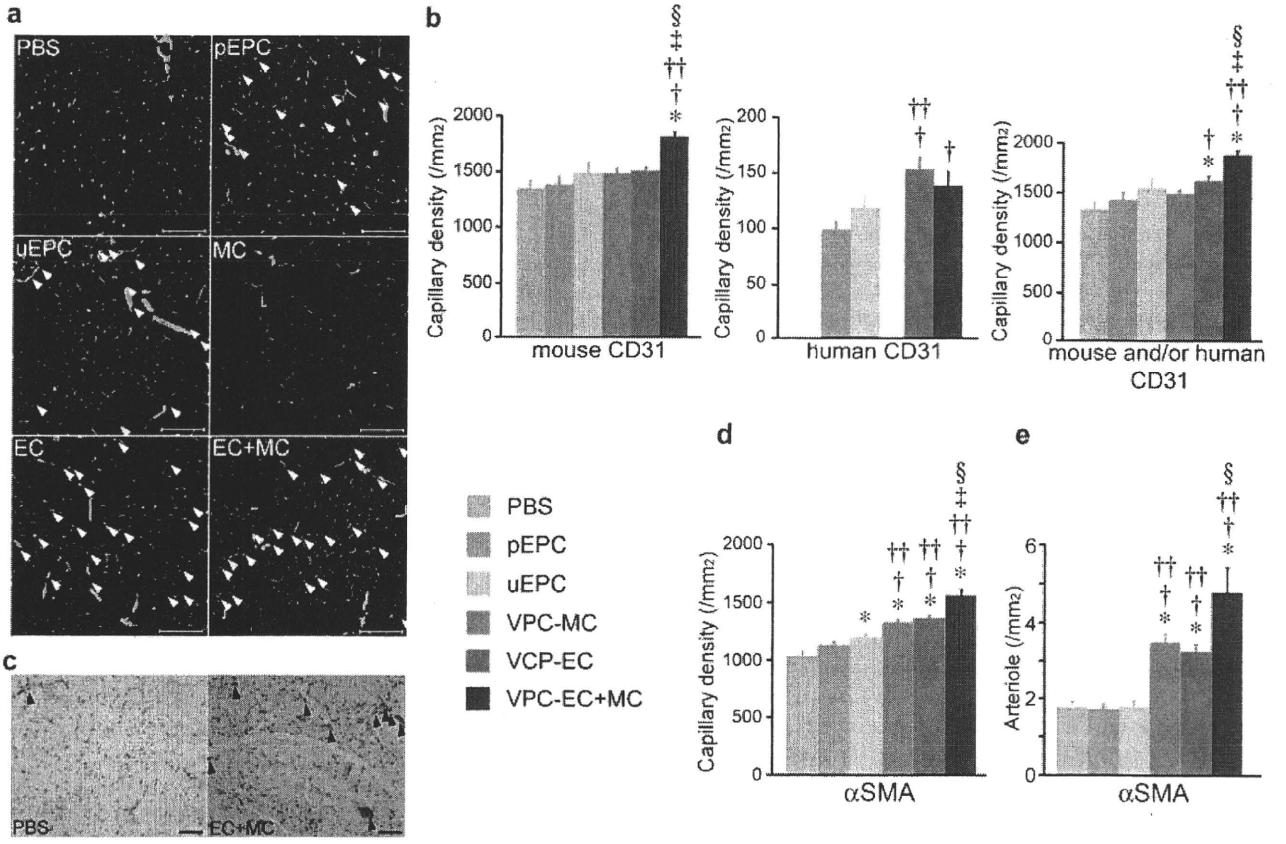

Figure 6. Immunohistochemical analysis of human VPC-derived vascular cells-transplanted murine hindlimb tissues. a) Representative fluorescent photographs of ischemic hindlimb stained for human (red) and mouse (green) CD31 at day 42. Overlapped-stained capillaries are shown in arrowhead. Scale bar: 100 μm. b) Quantitative analysis of the endothelial cell marker positive capillary density in ischemic hindlimbs at day 42. c) Representative αSMA immunostaining (brown) of ischemic hindlimbs at day 42. Scale bar. 100 μm. d) Quantitative analysis of αSMA positive capillary density in ischemic hindlimbs at day 42. e) Quantitative analysis of αSMA positive arterioles (black arrowhead) at day 42. *$P<0.05$ vs. control, †$P<0.05$ vs. pEPC, ††$P<0.05$ vs. uEPC, ‡$P<0.05$ vs. MC, §$P<0.05$ vs. EC.
doi:10.1371/journal.pone.0001666.g006

regeneration, and these MC could make mature blood vessels with adequate MC coating.

VEGFR2 is one of the most specific markers involved in the earliest stage of vascular endothelial and hematopoietic differentiation [14]. Recent reports suggest that VEGFR2$^+$ mesodermal progenitor cells also contribute muscle lineages including vascular smooth, skeletal, and cardiac muscles [1,15]. This evidence indicates the possibility that human VPC-derived MC, which were expanded from VEGFR2$^+$TRA1$^-$VE-cadherin$^-$ cells, might contain skeletal or cardiac muscle cells. However, 40-cycle RT-PCR was confirmed negative for skeletal and cardiac specific markers in expanded human VPC-derived MC. We cultured VPC-derived MC on dishes coated with collagen type IV, which is the major component of basement membrane. Previous reports described that basement membrane played an essential role in endothelial and smooth muscle cell differentiation [16]. Recently, Xiao et al. demonstrated that pretreatment of mouse ES cells with antibodies against collagen IV significantly inhibited smooth muscle cell differentiation [17]. They also demonstrated PDGF receptor-β signaling pathway plays a crucial role in ES cell-derived smooth muscle cell differentiation using PDGF receptor-β siRNA knockdown studies. Therefore, we suspected that, under the presence of collagen type IV and PDGF-BB, our human VPC-derived VE-cadherin negative cells could only differentiate to MC.

Human VPC-derived EC+MC-transplanted KSN nude mice showed considerable blood flow recovery, which led to more than 1.2 in the perfusion ratio of ischemic/non-ischemic limb. When we transplanted human VPC-derived vascular cells to immunosuppressed C57BL/6 mice, the perfusion ratio elevated to nearly 1 (data not shown). Therefore, the tendency of the blood flow recovery in C57BL/6 mice was consistent with the data of KSN nude mice, the absolute value of blood flow ratio after hindlimb ligation was different. Because both KSN nude and C57BL/6 mice received the same procedure for hindlimb ischemia, the degree of perfusion recovery after induction of hindlimb ischemia between these mice might reflect their difference in genetic background for angiogenesis, as reported by Fukino et al [18]. They demonstrated that the VEGF and VEGFR1/2 expression in response to ischemia was impaired in BALB/c mice, compared to other mouse strains (i.e, C57BL/6J or C3H/He mice). These results indicate that, because of the difference in genetic background, spontaneous collateral formation might be accelerated in our KSN nude mice compared to other strain mice.

In transplantation experiments, the number of mouse and/or human CD31 and mouse CD31-positive capillary density in the EC group was 1601.4±51.4/mm^2 and 1470.1±41.6/mm2, respectively. This difference in capillary density (1601.4–1470.1 = 131.3) was consistent with the number of human CD31-positive capillary density (149.9±12.3/mm^2). However,

compared to the EC group, the EC+MC group showed significant augmentation in mouse and/or human CD31 positive capillary density without the increase of human CD31 positive capillary density. One possible reason for this discrepancy is paracrine effects of transplanted human VPC-derived vascular cells might accelerate angiogenesis in ischemic tissues. We demonstrated that cultured human VPC-derived vascular cells expressed several angiogenic factors including VEGF, bFGF, HGF and PDGF-BB, and the release of VEGF from human VPC-derived vascular cells was significantly upregulated after transplantation (data not shown) [4]. Therefore, in addition to the structural contribution of transplanted human VPC-derived vascular cells into the host vascular network, the paracrine effects of these cells might enhance vascular regeneration in tissue ischemia.

Several reports described the contribution of pEPC or uEPC to neovascularization in tissue ischemia [6,7]. However, it has not been clearly demonstrated whether transplanted EPC augment neovascularization through differentiation and proliferation into mature EC or indirectly through paracrine stimulation of resident EC proliferation. Rehamn et al. demonstrated that the majority of pEPC, which were positive for acLDL and ulex-lectin, expressed monocyte/macrophage markers, and only a minority cell fraction expressed the specific endothelial or stem/progenitor markers [8]. They also demonstrated that pEPC did not proliferate, but released several potent angiogenic growth factors. In this study, we confirmed that a low percentage of cultured pEPC and uEPC expressed endothelial makers. A considerable number of pEPC or uEPC were localized inside the capillary lumen, not in the vessel wall. In addition, we found that VEGF mRNA expression in transplanted EPC was significantly higher compared with before transplantation (data not shown). These results suggest that the majority of EPC might have little ability to proliferate or differentiate to endothelial linage, and their angiogenic effects could be attributed to angiogenic factors secreted from transplanted EPC.

In conclusion, we have shown that human VPC-derived cells could effectively differentiate and be expanded to EC and MC. Combined transplantation of these "immature" VPC-derived vascular cells, unlike "mature" somatic EC and MC, augmented reparative neovascularization and contributed to make newly formed vessels in the murine hindlimb ischemia model far more effectively compared to EPC transplantation. Thus, human ES cells-derived EC and MC can be used as the new promising cell source for therapeutic vascular regeneration in patients with tissue ischemia in order to realize a novel combined stem cell therapy.

Materials and Methods

Differentiation of Human VPC-derived EC and MC

Maintenance of human ES cell line (HES3) was as previously described [19]. To induce VPC, undifferentiated ES cells were cultured on an OP9 feeder cell line as reported [3,4]. To obtain human VPC-derived EC, VEGFR2$^+$TRA1$^-$VE-cadherin$^+$ cells were sorted by fluorescence activated cell sorter (FACSAria; Becton Dickinson, Bedford, MA) at day 10 of differentiation, and cultured on type IV collagen-coated dishes (Becton Dickinson) in the presence of 10% FCS and 50ng/ml VEGF (human VEGF165, Peprotech Inc, Rocky Hill, NJ). After 6 passages of these cells, we re-sorted VE-cadherin$^+$ cells for transplantation of human VPC-derived EC. To expand human VPC-derived MC, sorted VEGFR2$^+$TRA1$^-$VE-cadherin$^-$ cells derived from VPC at day 8 were re-cultured on type IV collagen-coated dishes with 1% FCS and 20ng/ml human PDGF-BB (Peprotech Inc). We transplanted these human VPC-derived MC after 6 passages.

Preparation of Human EPC

Peripheral MNC-derived EPC (pEPC) were obtained from healthy volunteer, as previously described [6]. To confirm EPC phenotype, cells were detached with cell dissociation buffer (Invitrogen, Carlsbad, CA) and incubated with DiI-labeled acLDL (Invitrogen) and FITC-labeled Ulex europaeus agglutinin I (ulex-lectin) (Sigma-Aldrich, St. Louis, MO) for 1 hour. These cells were analyzed by FACSAria to be confirmed as EPC [6,8].

Umbilical cord blood-derived CD34$^+$ EPC (uEPC) were isolated from human umbilical cord blood, which were obtained from Cell Bank, RIKEN BioResource Center (Tukuba, Japan). CD34$^+$ cells were separated by a magnetic bead separation method using autoMACS system with direct CD34$^+$ progenitor cell isolation kit (Miltenyi Biotec GmbH, Gladbach, Germany) [7]. Protocols for using human umbilical cord blood were approved by the Ethics Committee of Kyoto University Graduate School of Medicine.

Characterization of VPC-derived Vascular Cells and EPC

To evaluate the surface marker phenotype of VPC-derived vascular cells and EPC, these cells were detached by cell dissociation buffer with or without collagenase (Wako Pure Chemical Industries, Osaka, Japan) and labeled for 15 minutes at 4°C with various fluorescence-conjugated monoclonal antibodies (Table 1) [20]. Cells were washed and analyzed on FACSAria flow cytometer with ≥30,000 events stored.

For the staining of cultured VPC-derived vascular cells on dishes, cells were stained with anti-human CD31 (WM59) (Becton Dickinson) antibody and several smooth muscle specific markers, as shown in Table 2. Cultured hAoSMC (Cambrex, East Rutherford, NJ) were used to obtain positive control staining.

For RT-PCR analysis, total RNA was prepared with RNeasy Mini Kit (QIAGEN Inc., Valencia, CA), and RT-PCR was performed by TaKaRa One Step RNA PCR Kit (TaKaRa Bio Inc., Otsu, Japan). Total RNA from human heart and skeletal muscle were purchased from Clontech (Mountain View, CA). Primers are listed in Table 3 [21–23].

Hindlimb Ischemia Model and Cell Transplantation

After 8-week-old male KSN/Slc nude mice (Japan SLC, Shizuoka, Japan) were anesthetized with pentobarbital (80mg/kg, i.p.), the right femoral vein was ligated. To transplant vascular cells intra-arterially, we injected these cells in 100 μl PBS into the right femoral artery. Immediately after the cell injection, the right femoral artery and vein were ligated and excised [24]. Animal procedures were performed according to Kyoto University standards for animal care.

Assessment of Transplanted Animals

The measurement of hindlimb blood flow was performed with a LDPI analyzer (Moor Instruments, Devon, United Kingdom), as previously described [24].

At arbitrary time points, biotin conjugated Griffonia simplicifolia lectin (GSL) I-isolectin B_4 (Vector Laboratories, Burlingame, CA) in 100 μl PBS was injected into the portal vein 15 minutes before sacrifice. Cryostat sections (10 μm thick) of the ischemic lower legs were stained with anti-mouse/human CD31 (clone WM59/Mec13.3) (Becton Dickinson) or anti-αSMA/human SM1 (clone 1A4/3F8) (DakoCytomation, Glostrup, Denmark/Yamasa Co., Tokyo, Japan) antibodies. For biotinylated isolectin B_4 staining to detect circulating vessels, sections were incubated with streptoavidin conjugated Alexa Fluor dye (Invitrogen).

Capillary densities were examined by counting the number of capillaries stained with anti-human and/or mouse CD31 or anti-

Table 1. Fluorescence-conjugated monoclonal antibodies used for FACS analysis

Antibody	Specificity	Clone	Conjugated fluorescence	Supplier
VEGF-R2	Endothelial cells	KM1998	Alexa Fluor 647	A generous gift of Prof. M. Shibuya, Tokyo University (Ref.20)
VE-cadherin	Endothelial cells	55-7H1	FITC or PE	Becton Dickinson, Bedford, MA
von Willebrand Factor (vWF)	Endothelial cells	2F2-A9	Alexa Fluor 488	Becton Dickinson, Bedford, MA
CD31 (PECAM1)	Endothelial cells or Monocytes	WM59	Alexa Fluor 488	eBioscience, San Diego, CA
CD105 (Endoglin)	Endothelial cells or Monocytes	266	Alexa Fluor 647	Becton Dickinson, Bedford, MA
CD11b (Mac1)	Monocytes	ICRF44	PE	eBioscience, San Diego, CA
CD11c	Monocytes	B-ly6	FITC	Becton Dickinson, Bedford, MA
CD14	Monocytes	M5E2	APC	Becton Dickinson, Bedford, MA
CD45	Panleukocytes	HI30	PE	Becton Dickinson, Bedford, MA
CD54 (ICAM-1)	Panleukocytes	581	PE	Becton Dickinson, Bedford, MA
AC133	Stem/Progenitor cells	AC133	PE	Miltenyi Biotec GmbH, Bergisch Gladbach, Germany
c-kit	Stem/Progenitor cells	YB5.B8	APC	Becton Dickinson, Bedford, MA
CD34	Stem/Progenitor cells	581	FITC	Becton Dickinson, Bedford, MA

doi:10.1371/journal.pone.0001666.t001

Table 2. Smooth muscle specific antibodies used for analysis

Antibody	Specificity	Clone	Supplier
Alpha smooth muscle actin (αSMA)	Human & mouse	1A4	DakoCytomation Denmark A/S, Glostrup, Denmark Sigma-Aldrich, St. Louis, MO
Calponin	Human	CALP	DakoCytomation Denmark A/S, Glostrup, Denmark
Smooth muscle myosin heavy chain 1 (SM1)	Human	3FB	Yamasa Co., Tokyo, Japan
Smooth muscle myosin heavy chain 2 (SM2)	Human & mouse	1G12	Yamasa Co., Tokyo, Japan

doi:10.1371/journal.pone.0001666.t002

Table 3. Primers for reverse transcription-polymerase chain reaction

Gene		Sequence	Length (bp)
Calponin[1]	Sense	5′-CTTCATGGACGGCCTCAAAGA-3′	713
	Antisense	5′-GTAGTTGTGTGCGTGGTGGTT-3′	
Smooth muscle myosin heavy chain 1 (SM1) and 2 (SM2)[1, 2]	Sense	5′-ATGAGGCCACGGAGAGCAACGA-3′	178 (SM1)
	Antisense	5′-CCATTGAAGTCTGCGTCTCGA-3′	217 (SM2)
h-caldesmon[1]	Sense	5′-AGACAAGGAAAGAGCTGAGGCA-3′	395
	Antisense	5′-GCTGCTTGTTACGTTTCTGCTC-3′	
Glyceraldehyde-3-phosphate dehydrogenase (GAPDH)[1]	Sense	5′-ACCACAGTCCATGCCATCAC-3′	452
	Antisense	5′-TCCACCACCCTGTTGCTGTA-3′	
Myogenin[3]	Sense	5′-GTGGGCGTGTAAGGTGTGTA-3′	141
	Antisense	5′-TGGTTGGGGTTGAGCAGGGT-3′	
MyoD[3]	Sense	5′-CCAAATGTAGCAGGTGTAAC-3′	142
	Antisense	5′-AGAGATAAATACAGCCCCAG-3′	
Cardiac troponin T (cTnT)[4]	Sense	5′-GGCAGCGGAAGAGGATGCTGAA-3′	150
	Antisense	5′-GAGGCACCAAGTTGGGCATGAACGA-3′	
Cardiac troponin I (cTnI)[4]	Sense	5′-CCCTGCACCAGCCCCAATCAGA-3′	250
	Antisense	5′-CGAAGCCCAGCCCGGTCAACT-3′	

[1]Ref. 21.
[2]We used a single pair of PCR primers that cover the sequence specific to SM2, because these two isoforms are produced from a single gene by alternative splicing.
[3]Ref. 22.
[4]Ref. 23.
doi:10.1371/journal.pone.0001666.t003

αSMA antibodies. Twenty (for CD31) or ten (for αSMA) random fields on two different sections (approximately 3mm apart) from each mouse were photographed and analyzed by NIH image as previously described [24].

Statistical Analysis

Results are presented as means±S.E.M. The serial changes of the hindlimb blood flow were assessed by repeated measures ANOVA, followed by Bonferoni's multiple comparison test. Comparisons among groups were tested by one-way ANOVA followed by Bonferoni's multiple comparison test. A P value <0.05 was considered significant.

References

1. Yamashita J, Itoh H, Hirashima M, Ogawa M, Nishikawa S, et al. (2000) Flk1-positive cells derived from embryonic stem cells serve as vascular progenitors. Nature 408: 92–96.
2. Yurugi-Kobayashi T, Itoh H, Yamashita J, Yamahara K, Hirai H, et al. (2003) Effective contribution of transplanted vascular progenitor cells derived from embryonic stem cells to adult neovascularization in proper differentiation stage. Blood 101: 2675–2678.
3. Sone M, Itoh H, Yamashita J, Yurugi-Kobayashi T, Suzuki Y, et al. (2003) Different differentiation kinetics of vascular progenitor cells in primate and mouse embryonic stem cells. Circulation 107: 2085–2088.
4. Sone M, Itoh H, Yamahara K, Yamashita JK, Yurugi-Kobayashi T, et al. (2007) Pathway for differentiation of human embryonic stem cells to vascular cell components and their potential for vascular regeneration. Arterioscler Thromb Vasc Biol 27: 2127–2134.
5. Asahara T, Murohara T, Sullivan A, Silver M, van der Zee R, et al. (1997) Isolation of putative progenitor endothelial cells for angiogenesis. Science 275: 964–967.
6. Kalka C, Masuda H, Takahashi T, Kalka-Moll WM, Silver M, et al. (2000) Transplantation of ex vivo expanded endothelial progenitor cells for therapeutic neovascularization. Proc Natl Acad Sci U S A 97: 3422–3427.
7. Murohara T, Ikeda H, Duan J, Shintani S, Sasaki K, et al. (2000) Transplanted cord blood-derived endothelial precursor cells augment postnatal neovascularization. J Clin Invest 105: 1527–1536.
8. Rehman J, Li J, Orschell CM, March KL (2003) Peripheral blood "endothelial progenitor cells" are derived from monocyte/macrophages and secrete angiogenic growth factors. Circulation 107: 1164–1169.
9. Fina L, Molgaard HV, Robertson D, Bradley NJ, Monaghan P, et al. (1990) Expression of the CD34 gene in vascular endothelial cells. Blood 75: 2417–2426.
10. Frid MG, Shekhonin BV, Koteliansky VE, Glukhova MA (1992) Phenotypic changes of human smooth muscle cells during development: late expression of heavy caldesmon and calponin. Dev Biol 153: 185–193.
11. Ferreira LS, Gerecht S, Shieh HF, Watson N, Rupnick MA, et al. (2007) Vascular progenitor cells isolated from human embryonic stem cells give rise to endothelial and smooth muscle like cells and form vascular networks in vivo. Circ Res 101: 286–294.
12. Chan-Ling T, Page MP, Gardiner T, Baxter L, Rosinova E, et al. (2004) Desmin ensheathment ratio as an indicator of vessel stability: evidence in normal development and in retinopathy of prematurity. Am J Pathol 165: 1301–1313.
13. Hughes S, Chan-Ling T (2004) Characterization of smooth muscle cell and pericyte differentiation in the rat retina in vivo. Invest Ophthalmol Vis Sci 45: 2795–2806.
14. Nishikawa SI, Nishikawa S, Hirashima M, Matsuyoshi N, Kodama H (1998) Progressive lineage analysis by cell sorting and culture identifies FLK1+VE-cadherin+ cells at a diverging point of endothelial and hemopoietic lineages. Development 125: 1747–1757.
15. Motoike T, Markham DW, Rossant J, Sato TN (2003) Evidence for novel fate of Flk1+ progenitor: contribution to muscle lineage. Genesis 35: 153–159.
16. Sakata N, Kawamura K, Takebayashi S (1990) Effects of collagen matrix on proliferation and differentiation of vascular smooth muscle cells in vitro. Exp Mol Pathol 52: 179–191.
17. Xiao Q, Zeng L, Zhang Z, Hu Y, Xu Q (2007) Stem cell-derived Sca-1+ progenitors differentiate into smooth muscle cells, which is mediated by collagen IV-integrin alpha1/beta1/alphav and PDGF receptor pathways. Am J Physiol Cell Physiol 292: C342–352.
18. Fukino K, Sata M, Seko Y, Hirata Y, Nagai R (2003) Genetic background influences therapeutic effectiveness of VEGF. Biochem Biophys Res Commun 310: 143–147.
19. Reubinoff BE, Pera MF, Fong CY, Trounson A, Bongso A (2000) Embryonic stem cell lines from human blastocysts: somatic differentiation in vitro. Nat Biotechnol 18: 399–404.
20. Sawano A, Iwai S, Sakurai Y, Ito M, Shitara K, et al. (2001) Flt-1, vascular endothelial growth factor receptor 1, is a novel cell surface marker for the lineage of monocyte-macrophages in humans. Blood 97: 785–791.
21. Miwa Y, Sasaguri T, Inoue H, Taba Y, Ishida A, et al. (2000) 15-Deoxy-Delta(12,14)-prostaglandin J(2) induces G(1) arrest and differentiation marker expression in vascular smooth muscle cells. Mol Pharmacol 58: 837–844.
22. Kato H, Ohta S, Koshida S, Narita T, Taga T, et al. (2003) Expression of pericyte, mesangium and muscle markers in malignant rhabdoid tumor cell lines: differentiation-induction using 5-azacytidine. Cancer Sci 94: 1059–1065.
23. Kehat I, Kenyagin-Karsenti D, Snir M, Segev H, Amit M, et al. (2001) Human embryonic stem cells can differentiate into myocytes with structural and functional properties of cardiomyocytes. J Clin Invest 108: 407–414.
24. Yamahara K, Itoh H, Chun TH, Ogawa Y, Yamashita J, et al. (2003) Significance and therapeutic potential of the natriuretic peptides/cGMP/cGMP-dependent protein kinase pathway in vascular regeneration. Proc Natl Acad Sci U S A 100: 3404–3409.

Acknowledgments

The human ES cells (HES3) were provided by ES Cell International Pre Ltd., Singapore.

Author Contributions

Conceived and designed the experiments: KY HI KN MS JY TY TC KH DT KM KP NO NS NT YF. Performed the experiments: KY MS KH. Analyzed the data: KY. Wrote the paper: KY HI.

EXPERIMENTAL CELL RESEARCH 314 (2008) 939–949

available at www.sciencedirect.com

ScienceDirect

www.elsevier.com/locate/yexcr

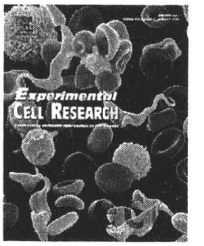

Research Article

Identification of adherens junction-associated GTPase activating proteins by the fluorescence localization-based expression cloning

Miho Matsuda[a,1,2], *Yuka Kobayashi*[a,1,3], *Sayuri Masuda*[a,b], *Makoto Adachi*[a], *Tsuyoshi Watanabe*[b], *Jun K. Yamashita*[c], *Eiichiro Nishi*[d], *Shoichiro Tsukita*[a], *Mikio Furuse*[b,*]

[a]*Department of Cell Biology, Graduate School of Medicine, Kyoto University, Yoshida-Konoe, Sakyo-ku, Kyoto 606-8501, Japan*
[b]*Division of Cell Biology, Department of Physiology and Cell Biology, Kobe University Graduate School of Medicine, 7-5-1 Kusunoki-cho, Chuo-ku, Kobe 650-0017, Japan*
[c]*Laboratory of Stem Cell Differentiation, Stem Cell Research Center, Institute of Frontier Medical Sciences, Kyoto University, 53 Kawahara-cho, Shogoin, Sakyo-ku, Kyoto 606-8507, Japan*
[d]*Molecular Pathology Unit, Horizontal Medical Research Organization, Graduate School of Medicine, Kyoto University, Yoshida-Konoe, Sakyo-ku, Kyoto 606-8501, Japan*

ARTICLE INFORMATION

Article Chronology:
Received 24 March 2007
Revised version received
19 October 2007
Accepted 12 November 2007
Available online 19 November 2007

Keywords:
Junctional complex
Adherens junctions
Tight junctions
FL-REX
GFP
GAP
ARHGAP12
SPAL3
Rap1

ABSTRACT

The junctional complex, including tight junctions (TJs), adherens junctions (AJs), and desmosomes, plays crucial roles in the structure and functions of epithelial cellular sheets. In this study, we evaluated the fluorescence localization-based retrovirus-mediated expression cloning (FL-REX) method as an approach to identify novel molecular components of TJs and AJs. Using an expression library of cDNA–GFP-fusions derived from mRNA of a mouse epithelial cell line, we confirmed that cDNAs for various known TJ- and AJ-components could be cloned in the FL-REX. Furthermore, cDNAs for ARHGAP12 and SPAL3, two putative GTPase activating proteins (GAPs) for small G proteins, were cloned as novel components of the junctional complex. Immunofluorescence staining using antibodies generated in-house demonstrated that these GAPs were localized at epithelial cell–cell junctions in various mouse tissues, and were specific to AJs when observed under confocal laser-scanning microscopy. These data suggest that FL-REX is a powerful tool to identify novel proteins localized at TJs and AJs.

* *Corresponding author.* Fax: +81 78 382 5805.
E-mail address: furuse@med.kobe-u.ac.jp (M. Furuse).
[1] These two authors contribute equally in this work.
[2] Present address: Laboratory of Molecular Genetics, NICHD, National Institute of Health, Bethesda, MD 20892, USA.
[3] Yuka Kobayashi's present address is Research Unit for Immune Tissue Engineering, Research Center for Allergy and Immunology, RIKEN Yokohama Institute,1-7-22 Suehiro-cho, Tsurumi,Yokohama 230-0045, Japan.

0014-4827/$ – see front matter © 2007 Elsevier Inc. All rights reserved.
doi:10.1016/j.yexcr.2007.11.009

Introduction

The junctional complex, which consists of tight junctions (TJs), adherens junctions (AJs), and desmosomes (DSs), is a hallmark of epithelial cell types in vertebrates [1]. The junctional complex plays crucial roles in mechanical adhesion between epithelial cells to form cellular sheets (AJs and DSs), as well as regulation of paracellular transport to maintain ionic homeostasis between different body compartments (TJs) [2–4,31]. Previous studies have identified a number of molecular constituents for each junction type in the junctional complex, enabling molecular characterization of the structure and function of each junction. One of the common features of these cell–cell junctions is the connection of adhesion molecules in the plasma membrane with cytoskeletons via cytoplasmic plaque proteins [2–4,31]. In addition to these structural proteins, a number of signaling molecules localized at the cytoplasmic region of the junctional complex are thought to be involved in the functional regulation of each cell–cell junction, cell growth, and morphogenesis of epithelial polarity [2–4,31].

An optimal approach to identify molecular constituents of each cell–cell junction is the purification of these structures followed by protein analyses of their components. Among the elements of the junctional complex, the purification of DSs from calf muzzles has been demonstrated, and various DS-associated proteins, including desmogleins and desmoplakins, have been identified from this DS fraction in one-dimensional SDS-PAGE [5,6]. In contrast, the purification of TJs and AJs was less successful [7,8], although alternatively, the production of monoclonal antibodies is a promising technique to identify the molecular constituents of these structures [9,10]. For example, several TJ-associated proteins including ZO-1 and occludin were discovered by the localization-based screening of monoclonal antibodies generated against a TJ-enriched plasma membrane fraction isolated from rodent or avian tissues [9,10]. However, a limitation of this approach is that it depends on the antigenicity, which cannot be controlled. In addition to biochemical and immunological approaches, searches for binding partners of cell–cell junction-associated proteins by co-precipitation and yeast two-hybrid screening have also identified many novel cell–cell junction-related molecules. Nevertheless, there are likely to be yet unidentified proteins localized at the junctional complex. Identification and characterization of these novel molecular components are important for further understanding of the structure and functional regulation of each junction at the molecular level.

To complement these biochemical and immunological approaches, the localization-based expression cloning would be useful to identify cDNAs for novel components of the junctional complex. In this 'visual screening' method, green fluorescent protein (GFP)-fused cDNA or genomic library is initially introduced into the cells. The cells in which exogenous GFP-fusion proteins are localized at certain cellular structures are then selected by fluorescence microscopy, and their cDNAs are cloned. This localization-based screening was first described in *Schizosaccharomyces pombe* [32], and then in mammalian cultured cells to identify a new type of nuclear envelope membrane protein [33]. Furthermore, Kitamura et al. developed the fluorescence localization-based retrovirus-mediated expression cloning (FL-REX) by the use of a retrovirus vector, which allows controllable introduction of cDNA libraries into cells with high-efficiency [11]. However, as of yet, reports on further applications of this method are limited [12].

In this study, we evaluated the FL-REX in obtaining cDNAs of novel molecular constituents localized at TJs and AJs in epithelial cells. We have confirmed that various cDNAs for known TJ- or AJ-associated proteins could be cloned in the FL-REX. Further, using this method we have identified two putative GTPase activating proteins (GAPs) for small G proteins as novel components of the junctional complex. Using in-house generated polyclonal antibodies (pAbs) for these GAPs, they were found to be localized at AJs in various epithelial tissues. These data suggest that FL-REX is a powerful tool to identify novel molecular constituents of the junctional complex.

Materials and methods

Cell culture and transfection

Epithelial cell lines, MDCK II, CSG120/7, and EpH4 were kindly provided by Dr. M. Murata (The University of Tokyo, Tokyo, Japan), Dr. W. Birchmeier (Max-Delbruck-Center for Molecular Medicine, Berlin, Germany), and Dr. E. Reichmann (University Children's Hospital Zurich, Zurich, Switzerland). A potent retrovirus packaging cell line, Plat-E [13], was kindly gifted by Dr. T. Kitamura (The University of Tokyo, Tokyo, Japan). All cells were grown in Dulbecco's modified Eagle's medium supplemented with 10% fetal calf serum. To establish the MDCK II cells competent to mouse retrovirus infection, the ecotropic mouse retrovirus receptor (EcoVR) cDNA (provided by Dr. T. Kitamura) was subcloned into pCAGGS-neodelEcoRI [14] and transfected to MDCK II cells with LipofectAMINE with Plus reagent (Invitrogen, Carlsbad, California, USA). One G418-resistant clone, MDCKIIVR20, was used for the expression cloning.

Construction of the cDNA library for FL-REX

A mouse retrovirus vector, pMX, was kindly provided by Dr. T. Kitamura. To avoid the background fluorescence of native GFP from the vector without cDNA insert in the cDNA–GFP-fusion library, we initially generated pMX-EGFPN-Met(–), a pMX-derived vector containing the EGFP sequence (CLONTCH) in which the ATG codon for the first methionine was deleted, and the EcoRI site with the DNA sequence encoding four glycines were inserted instead. For the construction of the cDNA library, poly(A) + RNA was isolated from CSG120/7 epithelial cells [15] using FastTrack (Invitrogen). The cDNA was synthesized from the poly(A) + RNA with random primers using Time Saver™ cDNA Synthesis Kit (Amersham, Mountain View, California, USA). The cDNA fragments longer than 1kb were size-fractionated from the agarose gel using GFX™ PCR DNA and Gel Band Purification Kit (GE Healthcare, Little Chalfont, Buckinghamshire, England) and were inserted into the EcoRI site of pMX-EGFPN-Met(–), upstream of EGFP cDNA. The ligated DNA was electroporated into DH5a competent cells (Electromax DH5a; Invitrogen) by Gene Pulser (BioRad, Hercules, California, USA). Plasmid DNA was purified after 12h culture

Table 1 – Known TJ- and AJ-associated proteins identified in the FL-REX in this study

Protein	Encoded (total) amino acids	Reported localization
Claudin-2*	1–207 (230)	TJ
Claudin-3*	2–211 (219)	TJ
Claudin-4*	1–189 (210)	TJ
Claudin-7*	1–197 (211)	TJ
CAR*	1–287 (365)	TJ
ZO-1	1–309 (1745)	TJ
ZO-2	1–486 (1167)	TJ
α-catenin	634–875 (906)	AJ
β-catenin	1–719 (781)	AJ
Plakoglobin*	82–472 (745)	AJ
α-actinin-4*	125–624 (912)	AJ
Shroom2	1–348 (1487)	AJ

*Multiple clones were obtained and their representative data presented.

in 200ml of LB medium. The resulting library contained 4.9 × 10^6 independent clones with an average insert size of 1.3kb. The cDNA library was then converted to the high titer retroviruses in Plat-E packaging cells as described previously [11].

Localization-based expression screening

MDCKIIVR20 cells were infected with the retrovirus library at ~ 20% infection efficiency as described previously [12]. After two days, infected cells were trypsinized, and the GFP-positive cells collected by fluorescence-activating cell sorting (FACS) and sparsely plated on glass-based dishes (IWAKI, Tokyo, Japan). 48–72h after plating the cells were scanned under an Olympus IX71 fluorescence microscope (Olympus, Tokyo, Japan), and cell colonies that contain cells with GFP signals of cell–cell junctions were marked. At the same time the surrounding colonies were scraped with needles under a phase contrast microscope and removed by aspiration. After 4–5 days expansion, the positive colonies were picked up, trypsinized, and replated on the glass-based dishes. Cell clones showing the junctional staining were then selected under a fluorescent microscope, picked up in the same way, and expanded to prepare their genomic DNAs which were used as a template for PCR to recover the integrated cDNA with two primers (GGTGGACCATCCTCTAGACT and GTCGCC-GTCCAGCTCGAC). By the use of cDNA databases, full-length cDNAs were cloned by RT-PCR from total RNA of EpH4 cells. In six experiments ~ 1.2 × 10^6 cells in total with GFP fluorescence were collected by FACS and subjected to the screening.

Antibodies

Bacterial expression constructs of the GST fusion proteins containing aa. 72–226 of ARHGAP12 and aa. 1040–1412 of SPAL3 were generated by subcloning the corresponding DNA fragments amplified by PCR into pGEX4T-1 (Amersham). Each fusion protein was then produced in *Escherichia coli*, purified with glutathione-Sepharose 4B beads (Amersham), and injected subcutaneously into rabbits to raise polyclonal antibodies (pAbs). The identical antigen regions of ARHGAP12 and SPAL3 were also subcloned into pMAL-c2 (New England Laboratory, Wobum, Massachusetts, USA) to produce maltose-

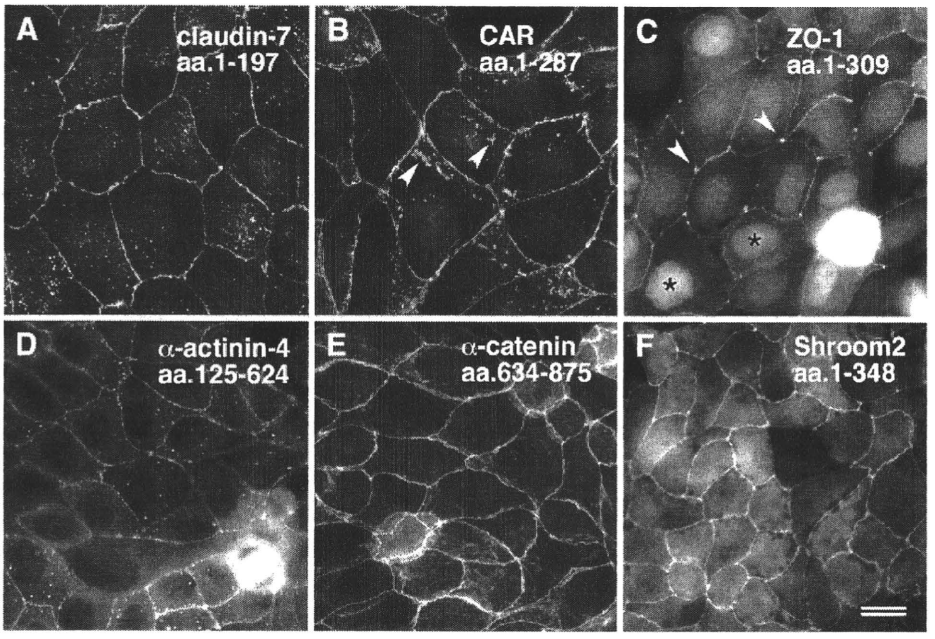

Fig. 1 – Fluorescent images of GFP-fusions localizing at cell–cell junctions in MDCK cells. In the FL-REX using a retrovirus expression library generated from CSG120/7 cells, various GFP-fusions with known TJ- and AJ-associated proteins were obtained. Six examples are shown. (A) claudin-7 (aa. 1–197), (B) CAR (aa. 1–287), (C) ZO-1 (aa. 1–309), (D) α-actinin-4 (aa. 125–624), (E) α-catenin (aa. 634–875), and (F) shroom2 (aa. 1–348). A GFP-fusion with CAR (aa. 1–287) localized at the lateral plasma membrane of MDCK cells as well as at cell–cell junctions as patches (arrowheads in B). A GFP-fusion with ZO-1 (aa. 1–309) was localized at nuclei and tricellular contacts (asterisks and arrowheads in C, respectively) in addition to cell–cell junctions. Scale bars; 10 μm.

binding protein fusions. For affinity purification of the pAbs, bacterial lysates of maltose-binding protein-ARHGAP12 and -SPAL3 fusion proteins were subjected to SDS-PAGE and blotted to nitrocellulose membranes. Membrane pieces blotted with the fusion proteins were incubated with the rabbit sera. After washing with PBS, the bound pAbs were collected by treatment of membranes with 0.2M citrate buffer (pH 2.3). Anti-E-cadherin mAb (ECCD-2) was kindly provided by Dr. M. Takeichi (Riken Center for Developmental Biology, Kobe, Japan). Anti-nectin-2 mAb was kindly provided from Dr. Y. Takai (Osaka University, Osaka, Japan). Anti-occludin mAb MOC37 was generated and characterized as described previously [35]. Anti-ZO-1 mAb R26.4 developed by Dr. D. Goodenough [9] was obtained from the Developmental Studies Hybridoma Bank, developed under the auspices of the NICHD and maintained by The University of Iowa, Department of Biological Sciences, Iowa City, IA 52242.

Immunofluorescence microscopy

Specimens for immunofluorescence microscopy were prepared as described previously [10]. To analyze the distribution of proteins in cultured cells, cells grown on glass coverslips were fixed with 1% formaldehyde in PBS for 15min at room temperature, permeabilized with 0.2% triton X-100 in PBS for 15min, and then washed three times with PBS. After blocking with 1% bovine serum albumin in PBS for 15min, samples were treated with primary antibodies and washed with PBS followed by treatment of secondary antibodies. For immunolocalization of proteins in mouse tissues, frozen sections (~ 5μm thick) of various mouse tissues embedded in O.C.T compound were cut in a cryostat, mounted on glass coverslips, air-dried, and fixed with 95% ethanol at – 20°C for 30min followed by 100% acetone at room temperature for 1min. After being washed with PBS, sections were blocked with 1% bovine serum albumin for 15min, treated with primary antibodies, and washed with PBS followed by treatment with secondary antibodies. After being washed with PBS, samples were mounted in 30% MOWIOL (CALBIOCHEM, La Jolla, California, USA). Specimens were observed using an Olympus IX70 fluorescence microscope (Olympus), a Zeiss Axio-phot photomicroscope, or Zeiss LSM510 confocal laser-scanning microscope (Carl Zeiss, Jena, Germany).

Results

Cloning of known cDNAs for TJ- and AJ-associated proteins in the FL-REX

In the present study, to improve the efficiency of the FL-REX for the screening and identification of novel components localized at the epithelial junctional complex, we adopted several modifications to reported methods. First, we created a cDNA–GFP-fusion library from the transcripts of CSG120/7 epithelial cells, a cell line derived from the mouse salivary gland. Secondly, to construct the retrovirus expression library for cDNA–GFP-fusions, the ATG codon of the first methionine of GFP in the vector was deleted in advance to avoid the background signal of native GFP from vectors without cDNAs, which are located upstream of GFP. This appeared to be effective as the ratio of cells with GFP signals in total cells infected with the retrovirus cDNA–GFP library was ~ 0.4% in this study, compared with 4% in the study by Nishimura et al., who preserved the initiation ATG of GFP [12]; infection efficiency approximately 20% in both studies. Next, cells were grown on glass-based culture plates instead of plastic ones to increase the detection sensitivity of GFP signal under the visual screening with an inverted fluorescence microscope.

Since TJs and AJs circumscribe the cells at the most apical part of the lateral plasma membrane, cells showing concentration of GFP-fusions into the apical cell–cell junction could be easily identified in the FL-REX. From ~ 1.2×10^6 GFP-positive cells collected by FACS in six experiments, we obtained a number of GFP-fusions with known TJ- and AJ-associated proteins (Table 1). The typical localization of these GFP-fusions

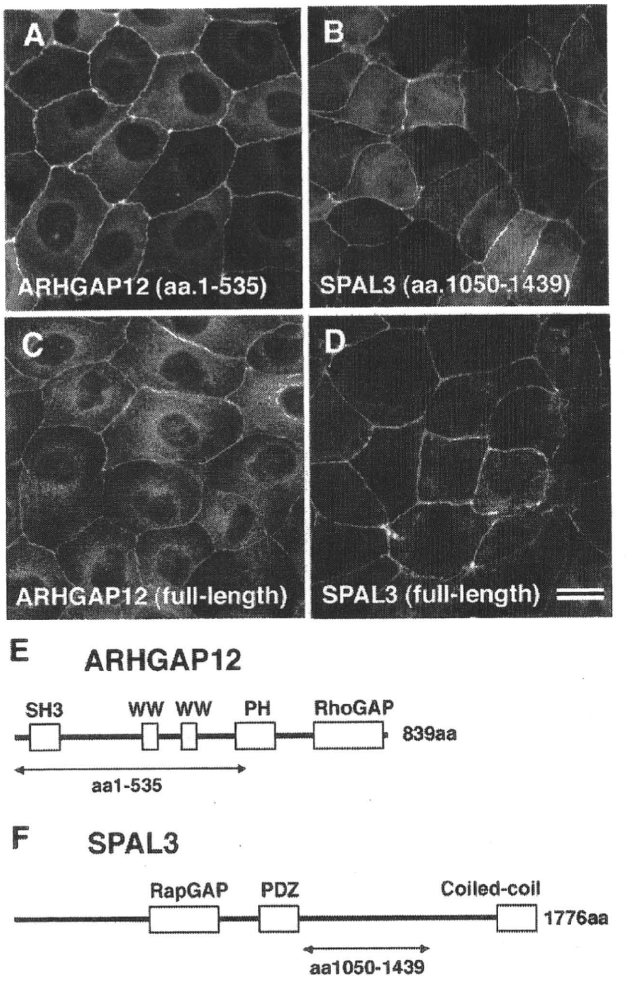

Fig. 2 – Identification of ARHGAP12 and SPAL3 as novel components of epithelial cell–cell junctions by the FL-REX. GFP-fusions with ARHGAP12 aa. 1–535 (A) and with SPAL3 aa. 1050–1439 (B) were concentrated at cell–cell junctions of MDCK cells in the FL-REX. Full-length ARHGAP12 (C) and SPAL3 (D) fused with GFP were also localized at cell–cell junctions. Domain structures of ARHGAP12 and SPAL3 were predicted by Pfam and SMART programs, and shown in (E) and (F) respectively. Scale bars; 10 μm.

in MDCK cells are shown in Fig. 1. The most abundant TJ proteins found by our screening were claudins, including claudin-2, -3, -4, and -7. cDNAs of claudins were obtained in every ~ 10^4 GFP-positive cells; this frequency was much higher than that of other junctional molecules (data not shown). cDNAs for other TJ-associated proteins CAR, ZO-1, and ZO-2 were also cloned in this screening. As cDNAs of known AJ-associated proteins, partial sequences of α-catenin, β-catenin, plakoglobin, α-actinin-4, and shroom2 were obtained.

Among these GFP-fusions, non-cell–cell junctional localizations were also observed. For example, CAR (aa. 1–287)–GFP-fusion was often detected as patches at the basolateral membrane of MDCK cells (Fig. 1B). In addition, ZO-1 (aa. 1–309)–GFP-fusion was localized at the nucleus and cytoplasm, and its concentration at tricellular contacts was remarkable (Fig. 1C). These localizations are likely to be artifacts as both proteins are known to be highly concentrated at tight junctions [7,34]. In contrast, strengthened localization of GFP-fusions into cell–cell junctions was also observed. α-catenin (aa. 634–875) showed a high concentration at the apical cell–cell junction (Fig. 1E), although endogenous α-catenin is distributed throughout the lateral plasma membrane including the apical cell–cell junction (data not shown).

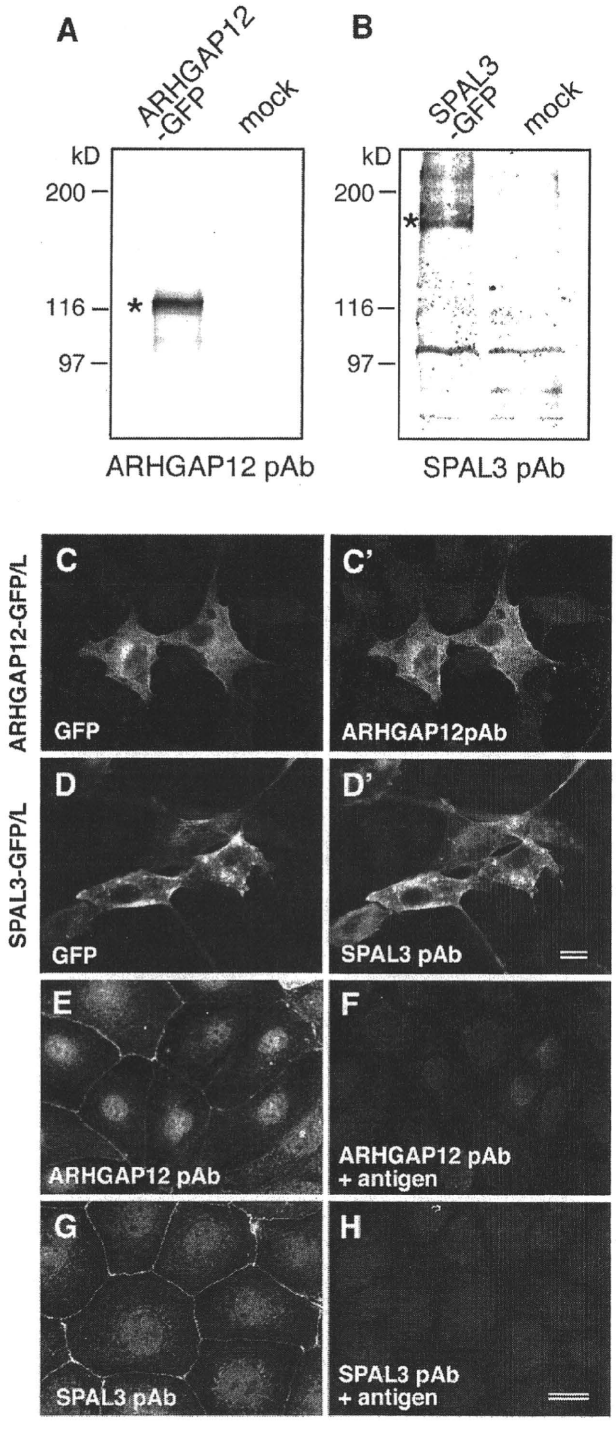

Fig. 3 – Evaluation of the specificity of anti-ARHGAP12 pAb and anti-SPAL3 pAb. (A), (B) Western blotting. Cell lysates of HEK293 cells expressing GFP-tagged full-length ARHGAP12 (ARHGAP12-GFP) or GFP-tagged SPAL3 aa. 341–1776 (SPAL3-GFP) were immunoblotted with anti-ARHGAP12 pAb (A) or anti-SPAL3 pAb (B). Asterisks indicate specific bands of ARHGAP12-GFP and SPAL3 aa. 341-1776-GFP respectively. Both antibodies did not recognize endogenous proteins in the lysate of parent HEK293 loaded on the same membranes (mock). (C–D') Immunostaining. ARHGAP12-GFP-expressing L cells (ARHGAP12-GFP/L) (C and C') and SPAL3-GFP-expressing L cells (SPAL3-GFP/L) (D and D') grown on coverslips were immunostained with anti-ARHGAP12 pAb (C') and anti-SPAL3 pAb (D'). The GFP signals from ARHGAP12-GFP (C) and SPAL3-GFP (D) completely overlapped with intensive signals of antibody staining. (E) Immunofluorescent image of EpH4 cells stained with anti-ARHGAP12 pAb. The junctional staining was undetectable after pretreatment of the primary antibody solution with an excess amount of the recombinant MBP-ARHGAP12 (aa. 72–226) protein (F). (G) The immunofluorescence image of EpH4 cells stained with anti-SPAL3 pAb. The junctional staining was undetectable after pretreatment of the primary antibody solution with an excess amount of the recombinant MBP-SPAL3 (aa. 1040–1412) fusion proteins (H). Scale bars; 10 μm.

Identification of ARHGAP12 and SPAL3, putative GTPase activating proteins for small G proteins, as components of epithelial cell–cell junctions

In the FL-REX screening based on the junctional localization, we have cloned GFP-fusions containing partial cDNAs for two putative GTPase activating proteins (GAPs) for small G proteins, neither of which have been reported to be localized at epithelial cell–cell junctions. One GFP-fusion contained aa. 1–535 of ARHGAP12 (GenBank accession no. NM029277), a putative Rho GTPase activating protein, whose cloning in human has been reported already (Fig. 2A) [16]. ARHGAP12 contains Src homology 3 (SH3) domain, two conserved tryptophans (WW) domain, pleckstrin homology (PH) domain, and Rho GAP domains in this order (Fig. 2E), and this overall domain structure is shared by other potential Rho GAPs including ARHGAP9 and ARHGAP15 [17]. Another GFP-fusion contained aa. 1050–1439 of SPAL3 (GenBank accession no. NM001081028) (Fig. 2C), a putative Rap GTPase activating protein. SPAL3 is closely related to SPAL (SPA-1 like-protein),

which was originally identified as a binding protein of PSD-95/SAP90, a scaffold protein of the post-synaptic density [18]. Similar to SPAL, SPAL3 contains Rap GAP, PDZ, and coiled–coil domains in this order (Fig. 2F). We then cloned full-length cDNAs of ARHGAP12 and SPAL3 in mice, and confirmed that their full-length constructs with GFP-tags were recruited to cell–cell contact sites when overexpressed in MDCK cells (Fig. 2B, D).

Since GFP-fusion with aa. 1–535 of ARHGAP12 containing SH3 domain and two WW domains localize at cell–cell junctions, we attempted to identify which domain is required for this localization. We constructed ARHGAP12-GFP mutants in which the SH3 domain (aa. 13–71) or two WW domains (aa. 263–388) were deleted, and produced MDCK cells stably expressing these deletion mutants. In fluorescence microscopy, however, neither of these constructs concentrated into cell–cell junctions (Fig. S1).

Generation of antibodies for ARHGAP12 and SPAL3

To examine the tissue expression and the subcellular localization of ARHGAP12 and SPAL3, we raised rabbit polyclonal antibodies for these proteins. In Western blotting of the membrane on which cell lysates of GFP-tagged ARHGAP12-overexpressing HEK293 cells were loaded, anti-ARHGAP12 antibody recognized a band of ~ 120kDa, which is consistent with the mass of molecular weights of GFP (27kDa) and ARHGAP12 (92kDa) (Fig. 3A). Similarly, in the lysates of HEK293 cells overexpressing GFP-tagged SPAL3 aa. 341–1776, anti-SPAL3 antibody recognized a band of ~ 180kDa, which is consistent with the mass of the putative molecular weights of GFP (27kDa) and SPAL3 aa. 341–1776 (158kDa) (Fig. 3B). Both antibodies could not detect endogenous proteins in the lysate of parent HEK293. To evaluate the ability of these antibodies for immunostaining, mouse L fibroblasts transiently transfected with expression vectors for GFP-tagged mouse ARHGAP12 or GFP-tagged SPAL3 were labeled with these antibodies. As shown in Fig. 3C–D', anti-ARHGAP12 antibody and anti-SPAL3 antibody intensively recognized only cells with GFP signals from GFP-ARHGAP12 and GFP-SPAL3 respectively. Moreover, when EpH4 cells were immunolabeled with these antibodies, the staining patterns of cell–cell junctions were observed around the cells (Fig. 3E, G). No staining was observed following pretreatment of primary antibodies with excess recombinant antigens, indicating that endogenous ARHGAP12 and SPAL3 are localized at cell–cell junctions in EpH4 epithelial cells (Fig. 3F, H). Neither anti-ARHGAP12 nor anti-SPAL3 antibodies we generated could detect endogenous ARHGAP12 or SPAL3 protein in EpH4 cells in Western blotting probably because of their weak reactivities to blotted proteins. However, the transcripts of both proteins were detected by RT-PCR in various mouse cultured cell lines including epithelial cells, fibroblasts, and teratocarcinoma cells such as EpH4, CSG120/7, L, NIH3T3, and F9 cells (data not shown).

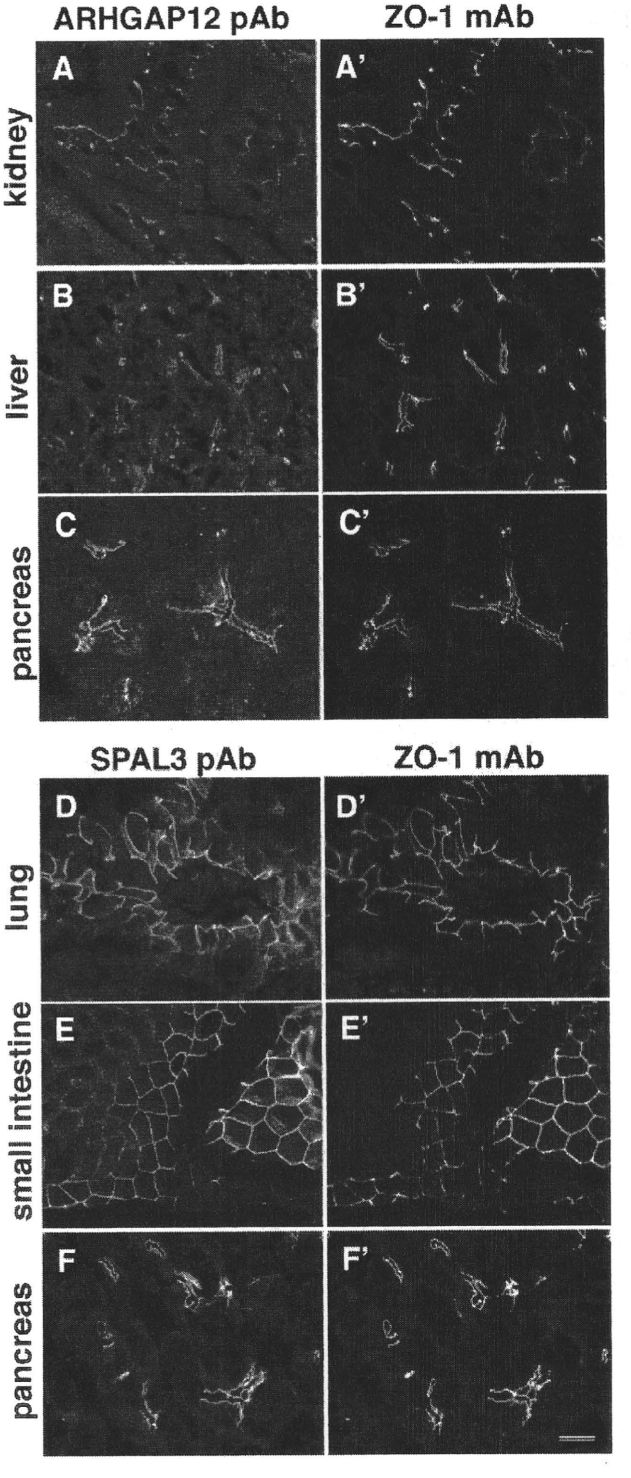

Fig. 4 – Immunolocalization of ARHGAP12 and SPAL3 in mouse tissues. Upper panel: frozen sections of mouse kidney, liver, and pancreas were double stained with anti-ARHGAP12 pAb (A–C) and anti-ZO-1 mAb (A'–C'). Fluorescent signals from ARHGAP12 and ZO-1 were mostly overlapped at cell–cell junctions of renal epithelial cells in the kidney (A and A'), hepatocytes in the liver (B and B'), and exocrine cells in the pancreas (C and C'). Lower panel: frozen sections of mouse lung, small intestine, and pancreas were double stained with anti-SPAL3 pAb (D–F) and anti-ZO-1 mAb (D'–F'). Fluorescent signals from SPAL3 and ZO-1 were mostly overlapped at cell–cell junctions of bronchial epithelial cells in the lung (D and D'), intestinal epithelial cells (E and E'), and exocrine cells in the pancreas (F and F'). Scale bars; 10 μm.

Subcellular localization of ARHGAP12 and SPAL3

Localization of ARHGAP12 and SPAL3 in mouse tissues was analyzed by immunofluorescence microscopy. Tissue sections were double-stained with either pAb of these GAPs and a mAb of ZO-1. ZO-1 is localized at TJs in epithelial cells, but is often used as a good marker for the junctional complex including TJs and AJs at the conventional fluorescence microscopy since its concentration into cell–cell contacts is remarkably clear compared with those of AJ-components such as E-cadherin and nectins, which are also localized at the basolateral membrane domain. As shown in Fig. 4, ARHGAP12 was localized at the junctional complex of tissues including the small intestine, the kidney, the salivary gland, and the liver. SPAL3 was detected at the junctional complex of various tissues including the lung, the small intestine, the kidney, and the salivary gland. In addition to the junctional complex, staining signals of ARHGAP12 and SPAL3 were detected in the cytoplasm and the basolateral membrane respectively, each of which appeared to be specific; pretreatment of the antibody with excess recombinant antigen of each protein abolished staining (data not shown). We observed no detectable ARHGAP12 or SPAL3 staining in blood vessels, suggesting that both GAPs are localized at cell–cell junctions in epithelial cells, but not in endothelial cells (data not shown).

To determine the precise localization of ARHGAP12 and SPAL3 within the junctional complex, double immunofluorescence staining of mouse small intestine was performed, and expression of these GAPs were compared with that of occludin [10], a marker for TJs, and E-cadherin and nectin-2 [19], markers for AJs, by confocal laser-scanning microscopy. As shown in Fig. 5, junctional expression of ARHGAP12 was more basal than that of occludin, and mostly overlapped with E-cadherin and nectin-2. SPAL3 showed the same distribution (Fig. 5). These results indicate that ARHGAP12 and SPAL3 are localized at AJs in the junctional complex of epithelial cells.

Localization of these GAPs at AJs suggested the possibility that these proteins are recruited to AJs by interacting with components of cadherin-mediated cell–cell adhesion. Thus, we examined the localization of these proteins in EL cells in immunofluorescence microscopy. EL cells were established from mouse L cells, which lack cadherin-mediated adhesion, by the stable introduction of E-cadherin [38]. EL cells exhibit E-cadherin-dependent cell–cell adhesion, and it has been reported that basic components of cadherin-mediated cell–cell adhesion such as E-cadherin, α-catenin, β-catenin are concentrated into cell–cell contact sites of EL cells [39]. In immunofluorescence staining, interestingly, endogenous SPAL3 was clearly colocalized with E-cadherin at cell–cell contact sites in EL cells whereas it was distributed in the cytoplasm in L cells (Fig. 6), suggesting the interaction of SPAL3 with basic components of cadherin-mediated cell–cell adhesion. The staining signal of EL cells with anti-ARHGAP12 pAb was very faint and its concentration at cell–cell contact sites was not detected (data not shown). Although this might be due to the low expression level of ARHGAP12 in EL cells, exogenous ARHGAP12-GFP expressed by transient transfection was not concentrated at cell–cell contact sites, or neither (data not shown).

Discussion

There is only one prior report of FL-REX used for the cDNA cloning of cell–cell junction-associated proteins [12]. In that study fluorescence-activating cell sorting (FACS) was introduced into the original FL-REX method, and the tight junction-associated protein identified JEAP was identified using a cDNA library generated from an endothelial cell line. However, further application of this method has not been reported. In this study, we adopted several modifications to previous methods to improve the efficiency of the screening, and suggest that the FL-REX is a useful tool to identify novel components of TJs and AJs as a complement to biochemical and immunological approaches.

The FL-REX has several advantages compared to biochemical approaches in the identification of novel proteins localizing at intercellular junctions, and also at various cellular structures. First, novel proteins can be obtained without purification of the cellular structure, which is often very difficult. Thus, the FL-REX is useful as far as cDNA libraries are available. Usually, only limited sources can be used for biochemical purifications of certain cellular structures. In contrast, the FL-REX is applicable to various cDNA sources, including most tissues and cell lines, as the established method for the cDNA library production is common to all sources. Secondly, since screening is performed in the native condition in living cells, proteins can be identified that are typically lost during biochemical isolation of cellular structures due to their low affinity with them. Previously reported isolation methods for intercellular junctions often expose the junctional membranes to unphysiological conditions, such as hypotonic buffer solution [7,8], in which some protein–protein interactions might be disrupted. These problems can be excluded in the FL-REX.

Conversely, there are also some problems in FL-REX. When expression cloning is performed with conventional cDNA libraries prepared from cellular poly(A)+RNAs, the efficiency of the cloning for given cDNAs is dependent on their expression levels, implying that cloning of cDNAs with low expression is difficult. Furthermore, localization domains should have correct conformations in GFP-fusions to show the correct subcellular localization. These limitations may account for our results demonstrating that claudins were cloned in our screening in much higher frequency than other junctional proteins. The construction of averaged cDNA libraries might overcome these problems to clone a different set of cDNAs. We have already confirmed that the use of cDNA libraries generated from cDNAs with different average sizes, or from different sources, provides different spectra of obtained cDNAs for AJ- and TJ- associated proteins (unpublished data), and further screening is ongoing in our laboratory.

In the present study, using the FL-REX method we cloned two putative GAPs for small G proteins, ARHGAP12 and SPAL3, as novel components of AJs. AJs circumscribe epithelial cells at their apical margins with actin filaments closely apposed to the membranes on the cytoplasmic side [1,2]. One of the important regulators of the actin cytoskeleton is the Rho family GTPase, which includes Rho, Rac, and Cdc42. Accumulating evidence suggests that this family are also involved in

the formation and function of AJs and TJs, probably through rearrangement of actin filaments [20,21]. The activities of Rho family GTPases are spatially and temporally controlled by guanine nucleotide exchange factor (GEF), which exchanges GDP for GTP, and GTPase activating protein (GAP), which accelerates the GTPase activity. To date, several GEFs and

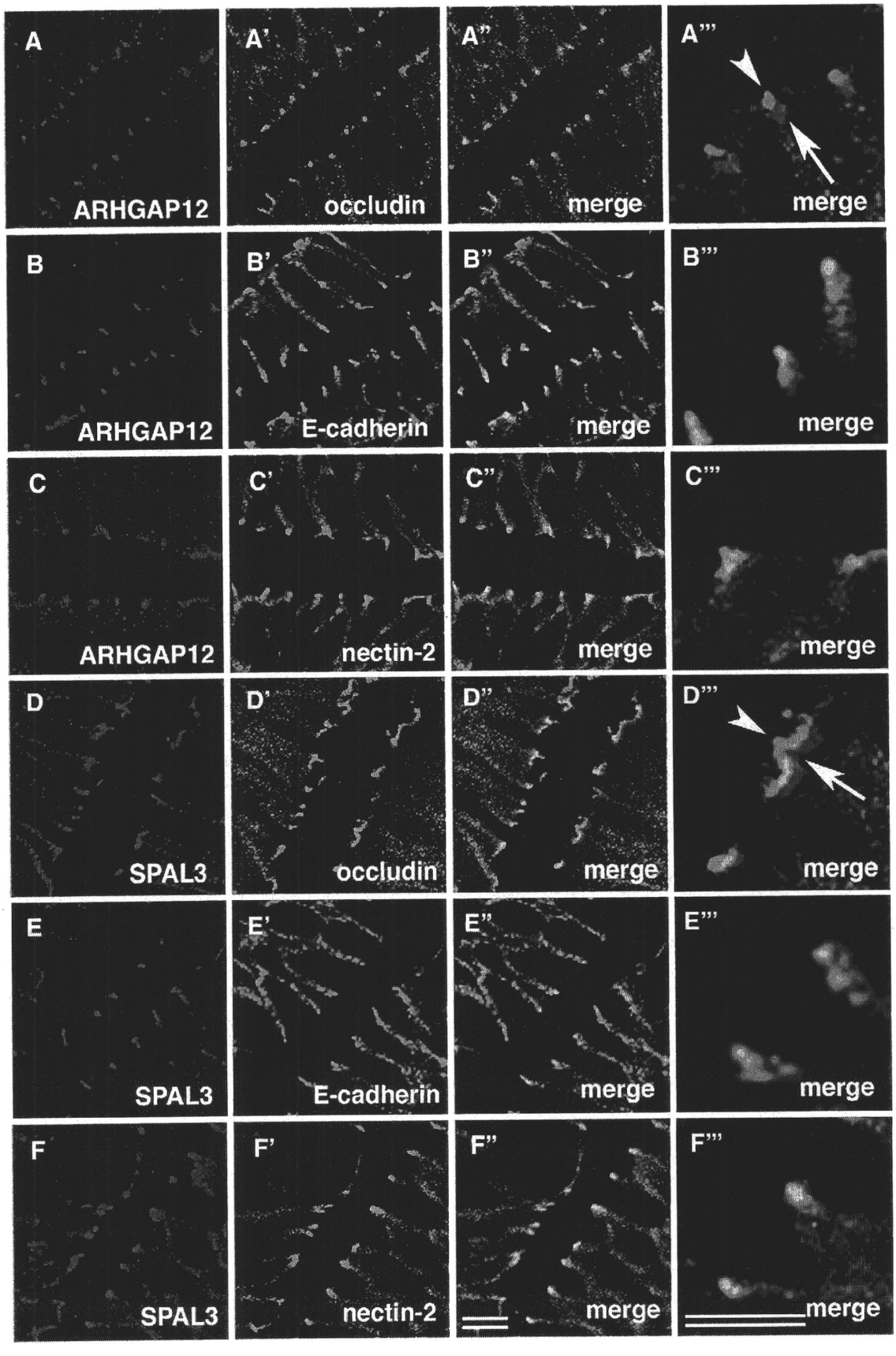

GAPs of Rho family GTPases have been demonstrated to be involved in the formation and configuration of TJs and AJs in epithelial cells [22–24].

ARHGAP12 is a member of closely related Rho GAPs including ARHGAP9 and ARHGAP15 [17]. ARHGAP9 demonstrated substantial GAP activity toward Cdc42Hs and Rac1, and its overexpression in human leukemia cells resulted in the repression of adhesion of cells to the extracellular matrix [25]. ARHGAP15 showed Rac1-specific GAP activity, and its overexpression in HeLa cells resulted in an increase in actin stress fibers and cell contraction [17]. Since ARHGAP12 is closely related to ARHGAP9 and 15, one possibility is that ARHGAP12 is involved in the regulation of AJ formation by spatially suppressing the activity of Rac1 and/or Cdc42 at AJs, although the specificity of GAPs has to be determined *in vivo* in each specific cell type. Alternatively ARHGAP12 may be involved in some other functions triggered by junction assembly. Since ARHGAP12 mutants, which lack either SH3 domain or WW domain, did not concentrate into cell–cell contacts in epithelial cells, both domains seems to be required for the localization of ARHGAP12 at AJs. It has been reported that SH3 domains of vinexin bind to vinculin [36] and lp-dlg [37], both of which are localized at AJs. Therefore, the SH3 domain of ARHGAP12 may also interact with these proteins. To date, the interaction of the WW domain with AJ-associated proteins has not been reported.

The sequence similarity of SPAL3 with those of SPA-1 and SPAL [18,26], both of which are Rap-GAPs, suggests that SPAL3 is also a Rap-specific GAP. Although Rap1 has been implicated in the control of integrin-mediated cell adhesion, recent evidence indicates that Rap1 also plays an important role in cadherin-mediated cell adhesion, including adherens junction formation [27]. Rap1 activity rescued Ras-induced disruption of cell–cell adhesion in MDCK cells and hepatocyte growth factor-induced cell scattering, suggesting that Rap1 positively regulates cadherin-based cell–cell adhesion [28]. Further, Hogan et al. reported that C3G, a Rap1GEF, interacts with the cytoplasmic domain of E-cadherin, and that ligation of the extracellular domain of E-cadherin enhances Rap1 activity, which in turn is necessary for the proper targeting of E-cadherin molecules to maturing cell–cell contacts [29]. Takai et al. have recently shown that Rap1 is also involved in adherens junction formation through the nectin–afadin system, another adhesion system of adherens junctions [30]. These observations suggest that SPAL3 may function in adherens junction formation by balancing the role of Rap1 by counteracting RapGEFs. The aa. 1050–1439 of SPAL3, which was required for localization at cell–cell contact sites in epithelial cells, does not contain any known domain structure (Fig. 2B, F). However, the fact that SPAL3 colocalized with E-cadherin at cell–cell contact sites in EL cells suggests that this region of SPAL3 interacts with the basic components of cadherin-mediated cell–cell adhesion, such as E-cadherin, α-catenin, β-catenin, and their binding proteins.

Although, so far, simple overexpression of ARHGAP12 and SPAL3 in EpH4 mouse epithelial cells seems not to affect cell morphology at the confluent condition (data not shown), these GAPs may be involved in the maturation of newly formed cell–cell contacts, the organization of actin stress fibers, or cell adhesion activity. Not only analyses along this line but also studies by knock down, overexpression of their dominant negative forms, and identification of binding partners will lead to better understanding their functions in epithelial AJs.

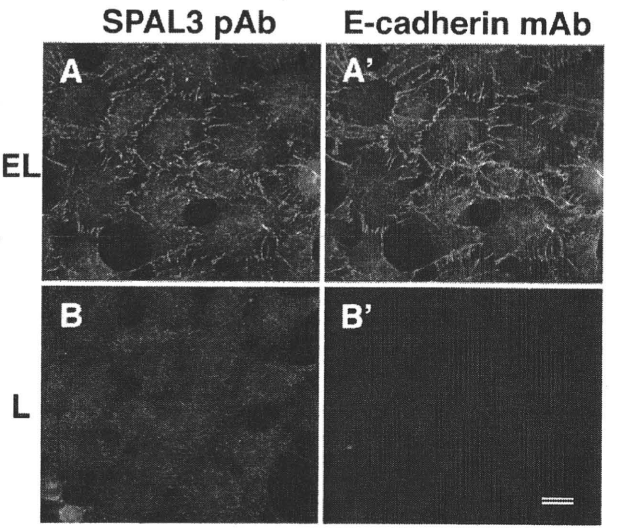

Fig. 6 – Localization of SPAL3 in L cells expressing E-cadherin. Double immunofluorescence staining of EL cells and L cells with anti-SPAL3 pAb (A, B) and anti-E cadherin mAb (A', B'). In EL cells, SPAL3 and E-cadherin were colocalized at cell–cell contact sites (A, A') whereas SPAL3 was distributed in the cytoplasm in L cells (B). Scale bars; 10 μm.

Acknowledgments

We would like to thank Dr. T. Kitamura for providing all reagents for the FL-REX, Dr. M. Takeichi for anti-E-cadherin mAb and EL

Fig. 5 – Distribution of ARHGAP12 and SPAL3 within the junctional complex. Upper panel: double immunofluorescence staining of mouse small intestine with anti-ARHGAP12 pAb and anti-occludin mAb (A–A'''), with anti-ARHGAP12 pAb and anti-E-cadherin mAb (B–B'''), or with anti-ARHGAP12 pAb and anti-nectin-2 mAb (C–C'''). In the merged image, ARHGAP12 (an arrow) was distributed more on the basal side of intestinal epithelial cells than occludin (an arrowhead) (A'' and A'''), whereas mostly colocalized with E-cadherin (B'' and B''') and nectin-2 (C'' and C''') at the junctional complex. Lower panel: double immunofluorescence staining of mouse small intestine with anti-SPAL3 pAb and anti-occludin mAb (D–D'''), with anti-SPAL3 pAb and anti-E-cadherin mAb (E–E'''), or with anti-SPAL3 pAb and anti-nectin-2 mAb (F–F'''). In the merged image, SPAL3 (an arrow) was distributed more on the basal side of intestinal epithelial cells than occludin (an arrowhead) (D'' and D'''), whereas colocalized with E-cadherin (E'' and E''') and nectin-2 (F'' and F'''). Occludin was used as a marker of TJs, wheareas E-cadherin and nectin-2 were used as markers of AJs. Scale bars; 10 μm.

cells, Dr. Y. Takai for anti-nectin-2 mAb, and Dr. T. Imai (KAN Research Institute, Ltd) and Ms. K. Umeda (Kumamoto University) for technical advice. We also thank Ms. C. Fujiwara for her excellent technical assistance, and all the members of Tsukita and Furuse laboratories for their helpful discussions.

This study was supported by a Grand-in-Aid for Scientific Research (B) from the Japan Society for the Promotion of Science and grants from Takeda Science Foundation and the Uehara Memorial Foundation to M.F.

Appendix A. Supplementary data

Supplementary data associated with this article can be found, in the online version, at doi:10.1016/j.yexcr.2007.11.009.

REFERENCES

[1] M.G. Farquhar, G.E. Palade, Junctional complexes in various epithelia, J. Cell Biol. 17 (1963) 375–412.
[2] A. Nagafuchi, Molecular architecture of adherens junctions, Curr. Opin. Cell Biol. 13 (2001) 600–603.
[3] D.R. Garrod, A.J. Merritt, Z. Nie, Desmosomal adhesion: structural basis, molecular mechanism and regulation, Mol. Membr. Biol. 19 (2002) 81–94.
[4] S. Tsukita, M. Furuse, M. Itoh, Multifunctional strands in tight junctions, Nat. Rev. Mol. Cell. Biol. 2 (2001) 285–2933.
[5] P. Drochmans, C. Freudenstein, J.C. Wanson, L. Laurent, T.W. Keenan, J. Stadler, R. Leloup, W.W. Franke, Structure and biochemical composition of desmosomes and tonofilaments isolated from calf muzzle epidermis, J. Cell Biol. 79 (1978) 427–443.
[6] G. Gorbslky, M.S. Steinberg, Isolation of the intercellular glycoprotein of desmosomes, J. Cell Biol. 90 (1981) 243–248.
[7] B.R. Stevenson, D.A. Goodenough, Zonulae occludentes in junctional complex-enriched fractions from mouse liver: preliminary morphological and biochemical characterization, J. Cell Biol. 98 (1984) 1209–1221.
[8] S.A. Tsukita, S.H. Tsukita, Isolation of cell–cell adherens junctions from rat liver, J. Cell Biol. 108 (1989) 31–41.
[9] B.R. Stevenson, J.D. Siliciano, M.S. Mooseker, D.A. Goodenough, Identification of ZO-1: a high molecular weight polypeptide associated with the tight junction (zonula occludens) in a variety of epithelia, J. Cell Biol. 03 (1986) 755–766.
[10] M. Furuse, T. Hirase, M. Itoh, A. Nagafuchi, S. Yonemura, S.A. Tsukita, S.H. Tsukita, Occludin: a novel integral membrane protein localizing at tight junctions, J. Cell Biol. 123 (1993) 1777–1788.
[11] K. Misawa, T. Nosaka, S. Morita, A. Kaneko, T. Nakahata, S. Asano, T. Kitamura, A method to identify cDNAs based on localization of green fluorescent protein fusion products, PNAS 97 (2000) 3062–3066.
[12] M. Nishimura, M. Kakizaki, Y. Ono, K. Morimoto, M. Takeuchi, Y. Inoue, T. Imai, Y. Takai, JEAP, a novel component of tight junctions in exocrine cells, J. Biol. Chem. 277 (2002) 5583–5587.
[13] S. Morita, T. Kojima, R. Kitamura, Plat-E: an efficient and stable system for transient packaging of retroviruses, Gene Ther. 7 (2000) 1063–1066.
[14] H. Niwa, K. Yamamura, J. Miyazaki, Efficient selection for high-expression transfectants with a novel eukaryotic vector, Gene 108 (1991) 193–200.
[15] M.A. Knowles, L.M. Franks, Stages in neoplastic transformation of adult epithelial cells by 7, 12-dimethylbenz(a)anthracene in vitro, Cancer Res. 37 (1977) 3917–3924.
[16] Z. Zhang, C. Wu, S. Wang, W. Huang, Z. Zhou, K. Ying, Y. Xie, Y. Mao, Cloning and characterization of ARHGAP12, a novel human rhoGAP gene, Int. J. Biochem. 34 (2002) 325–331.
[17] M.L. Seoh, C.H. Ng, J. Yong, L. Lim, T. Leung, ArhGAP15, a novel human RacGAP protein with GTPase binding property, FEBS Lett. 539 (2003) 131–137.
[18] B.C. Roy, K. Kohu, K. Matsuura, H. Yanai, T. Akiyama, SPAL, a Rap-specific GTPase activating protein, is present in the NMDA receptor-PSD-95 complex in the hippocampus, Genes Cells 7 (2002) 607–617.
[19] K. Takahashi, H. Nakanishi, M. Miyahara, K. Mandai, K. Satoh, A. Satoh, H. Nishioka, J. Aoki, A. Nomoto, A. Mizoguchi, Y. Takai, Nectin/PRR: an immunoglobulin-like cell adhesion molecule recruited to cadherin-based adherens junctions through interaction with afadin, aPDZ domain-containing protein, J. Cell Biol. 145 (1999) 539–549.
[20] K. Takaishi, T. Sasaki, H. Kotani, H. Nishioka, Y. Takai, Regulation of cell–cell adhesion by Rac and Rho small G proteins in MDCK cells, J. Cell Biol. 139 (1997) 1047–1059.
[21] T. Jou, E.E. Schneeberger, W.J. Nelson, Structural and functional regulation of tight junctions by RhoA and Rac1 small GTPases, J. Cell Biol. 142 (1998) 101–115.
[22] A.E. Mertens, T.P. Rygiel, C. Olivo, R. van der Kammen, J.G. Collard, The Rac activator Tiam1 controls tight junction biogenesis in keratinocytes through binding to and activation of the Par polarity complex, J. Cell Biol. 170 (2005) 1029–1037.
[23] T. Otani, T. Ichii, S. Aono, M. Takeichi, Cdc42 GEF Tuba regulates the junctional configuration of simple epithelial cells, J. Cell Biol. 175 (2006) 135–146.
[24] C.D. Wells, J.P. Fawcett, A. Traweger, Y. Yamanaka, M. Goudreault, K. Elder, S. Kulkarni, G. Gish, C. Virag, C. Lim, K. Colwill, A. Starostine, P. Metalnikov, T. Pawson, A Rich1/Amot complex regulates the Cdc42 GTPase and apical-polarity proteins in epithelial cells, Cell 125 (2006) 535–548.
[25] Y. Furukawa, T. Kawase, Y. Daigo, T. Nishiwaki, H. Ishiguro, M. Takahashi, J. Kitayama, Y. Nakamura, Isolation of a novel human gene ARHGAP9, encoding a Rho-GTPase activating protein, Biochem. Biophys. Res. Commun. 284 (2001) 643–649.
[26] N. Tsukamokto, M. Hattori, H. Yang, J.L. Bos, N. Minato, Rap1 GTPase-activating proteins SPA-1 negatively regulates cell adhesion, J. Biol. Chem. 274 (1999) 18463–18469.
[27] M.R.H. Kooistra, N. Dube, J.L. Bos, Rap1: a key regulator in cell–cell junction formation, J. Cell Sci. 120 (2007) 17–22.
[28] L.S. Price, A. Hajdo-Milasinovic, J. Zhao, F.J.T. Zwarkruis, J.G. Collard, J.L. Bos, Rap1 regulates E-cadherin-mediated cell–cell adhesion, J. Biol. Chem. 279 (2004) 35127–35132.
[29] C. Hogan, N. Serpente, P. Cogram, C.R. Hosking, C.U. Bialucha, S.M. Feller, V.M. Braga, W. Birchmeier, Y. Fujita, Rap1 regulates the formation E-cadherin-based cell–cell contacts, Mol. Cell Biol. 24 (2004) 6690–6700.
[30] T. Fukuyama, H. Ogita, T. Kawakatsu, T. Fukuhara, T. Yamada, T. Sato, K. Shimizu, T. Nakamura, M. Matsuda, Y. Takai, J. Biol. Chem. 280 (2005) 815–825.
[31] S. Aijaz, M.S. Balda, K. Matter, Tight junctions: molecular architecture and function, Int. Rev. Cytol. 248 (2006) 261–298.
[32] K.E. Sawin, P. Nurse, Identification of fission yeast nuclear markers using random polypeptide fusions with green fluorescent protein, Proc. Natl. Acad. Sci. U. S. A. 94 (1996) 15146–15151.
[33] M.M. Rolls, P.A. Stein, S.S. Taylor, E. Ha, F. McKeon, T.A. Rapoport, A visual screening of a GFP-fusion library identifies a new type of nuclear envelope membrane protein, J. Cell Biol. 146 (1999) 29–44.
[34] E. Raschperger, J. Thyberg, S. Pettersson, L. Philipson, J. Fuxe, R.F. Pettersson, The coxackie- and adenovirus receptor (CAR) is an in vivo marker for epithelial tight junctions, with a potential role in regulating permeability and tissue homeostasis, Exp. Cell Res. 312 (2006) 1566–1580.

[35] M. Saitou, Y. Ando-Akatsuka, M. Itoh, M. Furuse, J. Inazawa, K. Fujimoto, S. Tsukita, Mammalian occludin in epithelial cells: its expression and subcellular distribution, Eur. J. Cell Biol. 73 (1997) 222–231.
[36] N. Kioka, S. Sakata, T. Kawauchi, T. Amachi, S.K. Akiyama, K. Okazaki, C. Yaen, K.M. Yamada, S. Aota, Vinexin: a novel vinculin-binding protein with multiple SH3 domains enhances actin cytoskeletal organization, J. Cell Biol. 144 (1999) 59–69.
[37] M. Wakabayashi, T. Ito, M. Mitsushima, S. Aizawa, K. Ueda, T. Amachi, N. Kioka, Interaction of Ip-dlg/KIAA0583, a membrane-associated guanylate kinase family protein, with vinexin and b-catenin at sites of cell–cell contact, J. Biol. Chem. 278 (2003) 21709–21714.
[38] A. Nagafuchi, Y. Shirayoshi, K. Okazaki, K. Yasuda, M. Takeichi, Transformation of cell adhesion properties by exogenously introduced E-cadherin cDNA, Nature 329 (1987) 341–343.
[39] A. Nagafuchi, M. Takeichi, S. Tsukita, The 102 kd cadherin-associated protein: similarity to vinculin and posttranscriptional regulation of expression, Cell 65 (1991) 849–857.

J Appl Physiol 104: 766–772, 2008.
First published January 10, 2008; doi:10.1152/japplphysiol.00870.2007.

Cyclic strain induces mouse embryonic stem cell differentiation into vascular smooth muscle cells by activating PDGF receptor β

Nobutaka Shimizu,[1,2]* Kimiko Yamamoto,[1,3]* Syotaro Obi,[1] Shinichiro Kumagaya,[1] Tomomi Masumura,[1] Yasumasa Shimano,[1] Keiji Naruse,[4] Jun K. Yamashita,[5] Takashi Igarashi,[2] and Joji Ando[1]

[1]*Department of Biomedical Engineering and* [2]*Department of Pediatrics, Graduate School of Medicine, University of Tokyo, Tokyo, Japan;* [3]*PRESTO, Japan Science and Technology Agency, Saitama, Japan;* [4]*Department of Cardiovascular Physiology, Graduate School of Medicine, Dentistry, and Pharmaceutical Sciences, Okayama University, Okayama, Japan;* [5]*Stem Cell Research Center, Institute for Frontier Medical Sciences, Kyoto University, Kyoto, Japan*

Submitted 13 August 2007; accepted in final form 22 December 2007

Shimizu N, Yamamoto K, Obi S, Kumagaya S, Masumura T, Shimano Y, Naruse K, Yamashita JK, Igarashi T, Ando J. Cyclic strain induces mouse embryonic stem cell differentiation into vascular smooth muscle cells by activating PDGF receptor β. *J Appl Physiol* 104: 766–772, 2008. First published January 10, 2008; doi:10.1152/japplphysiol.00870.2007.—Embryonic stem (ES) cells are exposed to fluid-mechanical forces, such as cyclic strain and shear stress, during the process of embryonic development but much remains to be elucidated concerning the role of fluid-mechanical forces in ES cell differentiation. Here, we show that cyclic strain induces vascular smooth muscle cell (VSMC) differentiation in murine ES cells. Flk-1-positive (Flk-1$^+$) ES cells seeded on flexible silicone membranes were subjected to controlled levels of cyclic strain and examined for changes in cell proliferation and expression of various cell lineage markers. When exposed to cyclic strain (4–12% strain, 1 Hz, 24 h), the Flk-1$^+$ ES cells significantly increased in cell number and became oriented perpendicular to the direction of strain. There were dose-dependent increases in the VSMC markers smooth muscle α-actin and smooth muscle-myosin heavy chain at both the protein and gene expression level in response to cyclic strain, whereas expression of the vascular endothelial cell marker Flk-1 decreased, and there were no changes in the other endothelial cell markers (Flt-1, VE-cadherin, and platelet endothelial cell adhesion molecule 1), the blood cell marker CD3, or the epithelial marker keratin. The PDGF receptor β (PDGFRβ) kinase inhibitor AG-1296 completely blocked the cyclic strain-induced increase in cell number and VSMC marker expression. Cyclic strain immediately caused phosphorylation of PDGFRβ in a dose-dependent manner, but neutralizing antibody against PDGF-BB did not block the PDGFRβ phosphorylation. These results suggest that cyclic strain activates PDGFRβ in a ligand-independent manner and that the activation plays a critical role in VSMC differentiation from Flk-1$^+$ ES cells.

hemodynamic force; biomechanics; blood vessel

EMBRYONIC STEM (ES) cells derived from the inner cell mass of a blastocyst stage embryo are able to differentiate into the three embryonic germ layers (endoderm, ectoderm, and mesoderm) and are thus able to produce virtually all types of somatic cells (5, 16). ES cells are considered a promising source of seed cells for tissue engineering (22), and a great effort has been made to develop methods of inducing ES cells to differentiate into various specialized cells (1, 14, 25, 31). Yamashita et al. (34) developed a method that uses cell growth factors to induce selective differentiation of ES cells into vascular cells. In this method, undifferentiated mouse ES cells are cultured on type IV collagen-coated dishes, and vascular endothelial growth factor (VEGF) receptor 2 (Flk-1)-positive (Flk-1$^+$) cells are isolated by flow cytometry sorting. Addition of VEGF to the cultures promotes endothelial differentiation, whereas mural cells, including vascular smooth muscle cells (VSMCs) and pericytes, are induced by platelet-derived growth factor-BB (PDGF-BB). The vascular cells derived from Flk-1$^+$ cells have been shown to contribute to the developing vasculature in vivo.

Adult blood vessel cells are known to alter their shape, function, and gene expression in response to fluid-mechanical forces, such as shear stress produced by flowing blood and cyclic strain generated by pulsatile changes in blood pressure (3). The vascular cell responses to mechanical forces are thought to play an important role in sustaining the homeostasis of the circulatory system and in blood flow-dependent phenomena, such as angiogenesis, vascular remodeling, and atherogenesis. Fluid-mechanical forces have recently been shown to control embryonic development and organogenesis: intracardiac fluid forces are essential for the formation of a functional heart in zebrafish embryos (7), and the direction of fluid flow on the node of mouse embryos determines left-right asymmetry in the body plan (19). Moreover, it is now clear that fluid-mechanical forces affect immature and undifferentiated cells, as well as adult cells. Our previous studies (32, 33) showed that shear stress induces selective differentiation by bone marrow-derived endothelial progenitor cells and Flk-1$^+$ ES cells into the vascular endothelial cell (EC) lineage in vitro.

The hemodynamics of the mammalian embryo has recently been analyzed. Jones et al. (10, 11) made quantitative flow measurements during early organogenesis in mouse embryos and detected laminar shear stress levels of between 0 and 5.5 dyn/cm^2 in embryos from 8.5 to 10.5 days postcoitum (dpc) and a heart rate ranging from about 80 to 100 beats/min. According to data obtained from rat and chick embryos, pressure levels in embryos are low, ~1–2 mmHg (8, 17). During the process of embryonic development, ES cells appear to be exposed to shear stress and cyclic strain generated by the beating heart. Cyclic strain and shear stress have both been recognized as important modulators of vascular cell function, including cell proliferation, apoptosis, differentiation, morphology, migration, and the secretion of various macromolecules (12). More recent studies have revealed that cyclic strain

* N. Shimizu and K. Yamamoto contributed equally to this work.

Address for reprint requests and other correspondence: J. Ando, Dept. of Biomedical Engineering, Graduate School of Medicine, Univ. of Tokyo, 7-3-1 Hongo, Bunkyo-ku, Tokyo 113-0033, Japan (e-mail: joji@m.u-tokyo.ac.jp).

The costs of publication of this article were defrayed in part by the payment of page charges. The article must therefore be hereby marked "*advertisement*" in accordance with 18 U.S.C. Section 1734 solely to indicate this fact.

affects ES cell differentiation. Schmelter et al. (28) demonstrated that static mechanical strain promotes cardiovascular differentiation by ES cells through the generation of reactive oxygen species. Saha et al. (26), on the other hand, showed that mechanical strain has an inhibitory effect on ES cell differentiation. Thus the role of fluid-mechanical forces in ES cell differentiation seems open to discussion.

In the present study, we investigated whether cyclic strain affects the differentiation of Flk-1^+ ES cell and, if so, which cell lineage they differentiate into. Mouse Flk-1^+ ES cells cultured on flexible silicone membranes were subjected to controlled levels of cyclic strain and examined for changes in the expression of various cell lineage markers. We also investigated the molecular mechanism involved in the effects of cyclic strain on Flk-1^+ ES cell differentiation in terms of PDGF receptor phosphorylation.

MATERIALS AND METHODS

Cell culture. MGZ5 ES cells [gift from H. Niwa (Riken, CDB, Kobe, Japan)] were maintained, differentiated, and cultured as previously described (32). The cells were initially maintained undifferentiated without a feeder layer on gelatin-coated tissue culture dishes in DMEM (IBL, Fujioka, Japan) containing 15% FBS (JRH Biosciences), 10^3 U/ml leukemia inhibitory factor (ESGRO Complete kit; Chemicon), 1× nonessential amino acid (ICN Pharmaceuticals), and 5×10^{-5} mol/l β-mercaptoethanol (Sigma). To initiate ES cell differentiation, trypsinized cells were plated on type IV collagen-coated Petri dishes (BD Falcon) and cultured without leukemia inhibitory factor in α-MEM (GIBCO) containing 10% FBS, 50 U/ml penicillin-streptomycin (ICN Pharmaceuticals), and 5×10^{-5} mol/l β-mercaptoethanol. On *day 4*, Flk-1^+ ES cells were isolated by standard immunomagnetic techniques (MACS kit; Miltenyi Biotech) using anti-mouse Flk-1 antibody (Clone Avas 12α1; Pharmingen) and plated in differentiation medium (α-MEM containing 10% FBS, 50 U/ml penicillin-streptomycin, and 5×10^{-5} mol/l β-mercaptoethanol) in silicon chambers. After culture for 3 days, cells became confluent and were used for experiments.

Cyclic strain experiments. Flk-1^+ ES cells were exposed to cyclic strain with a uniaxial mechanical strain-loading device, as described previously (30). Briefly, type IV collagen-coated polydimethylsiloxane chambers in which the cells were cultured were fixed in a cyclic strain-loading device (STREX ST-140; Strex, Osaka, Japan). One end of the chamber was firmly attached to the fixed frame, and the other end of the chamber was fixed to the movable frame connected to a motor-driven shaft. The amplitude and frequency of stretching were controlled by a programmable microcomputer, and cyclic strain in the 2–12% range with 1 Hz was used in the present study. The polydimethylsiloxane membrane (32 mm × 32 mm) was uniaxially and uniformly stretched over the entire membrane area, except at both lateral edges (2–3 mm in width), where the strain was slightly lower than the amount applied; i.e., the difference between the lateral edges and other areas was no more than one-tenth of that applied. All experiments were performed at 37°C in a CO_2 incubator.

Immunohistochemistry. Cells were fixed with 4% paraformaldehyde (Sigma), permeabilized with 0.1% Triton X-100 (Sigma), and maintained in 1% normal BSA (Sigma) to block nonspecific protein binding sites. The cells were incubated with monoclonal antibodies against platelet endothelial cell adhesion molecule 1 (PECAM-1; Pharmingen) and then with monoclonal antibody against smooth muscle α-actin (SM α-actin; Sigma). After they were washed, cells were incubated with a secondary antibody (Alexa Fluor 488 goat anti-rat IgG or Alexa Fluor 594 goat anti-mouse IgG; Molecular Probes) at a dilution of 1:500. The cell nuclei were stained with 4′,6-diamidino-2-phenylindole (Sigma). Stained cells were photographed through a confocal laser scanning microscope (Leica), and all images were imported into Adobe Photoshop as JPEGs for contrast manipulation and figure assembly.

Western blot analysis. Western blot analyses were performed as previously described (32). Briefly, cells were dissolved in lysis buffer containing a 0.1% protease inhibitor mixture (Sigma) and centrifuged at 2.6×10^4 *g* for 30 min. The protein concentration of the lysate was determined with a protein assay kit (Bio-Rad). Equal amounts of protein were dissolved in SDS-PAGE sample buffer, separated by SDS-PAGE, transferred to Immobilon membranes (Millipore), and incubated with antibodies against SM α-actin or smooth muscle myosin heavy chain (SM-MHC; Biomedical Technologies). Anti-mouse PDGF receptor β (PDGFRβ) phosphospecific antibody (pY857; BD Pharmingen) was used for the analysis of PDGFRβ phosphorylation. After they were washed and incubated with horseradish peroxidase-linked anti-mouse or anti-rabbit IgG, immunoreactive proteins were visualized with the enhanced chemiluminescence plus detection system (Amersham) and GS363 molecular imager system (Bio-Rad).

Flow cytometry. Expression of various cell lineage marker proteins was measured by flow cytometry. Cells were detached from the dishes by incubation at room temperature for 15 min in PBS supplemented with 1 mM EDTA (Sigma) and then suspended in PBS with 10% FBS. A total of 200,000 cells were then incubated for 60 min at 4°C with monoclonal antibodies against the EC markers, including the VEGF receptors Flk-1 (Pharmingen) and Flt-1 (Chemicon), and the intercellular adhesion molecules VE-cadherin (Pharmingen) and PECAM-1, the blood cell marker T3 antigen (CD3; Pharmingen), and the epithelial cell marker keratin (NeoMarkers). Next, the cells were incubated for 60 min at 4°C with Alexa Fluor 488 goat anti-mouse IgG (Molecular Probes) and analyzed by fluorescence-activated cell sorting (Becton Dickinson). Histograms of cell number vs. logarithmic fluorescence intensity were recorded for 20,000 cells per sample. Background fluorescence was obtained from the negative control cells stained with the secondary antibody and subtracted from the mean fluorescence of the specific staining patterns. The expression level of each antigen was expressed as the mean channel fluorescence.

Real-time PCR analysis. Total RNA samples were prepared from cells with ISOGEN (Nippon Gene, Tokyo, Japan), and first-strand cDNAs were generated by using Moloney murine leukemia virus reverse transcriptase (Roche) and RNA primed with oligo(dT) primer. After reverse transcription of the RNA into cDNA, real-time PCR was used to monitor gene expression with a Smart Cycler (Cepheid) according to the standard procedure. PCR was performed with a Takara EX *Taq* R-PCR version (Takara) and the primer pairs shown in Table 1. The temperature profile consisted of initial denaturation for 30 s at 95°C followed by 35 cycles of denaturation at 95°C for 15 s, annealing at 60°C for 15 s, elongation at 72°C, and fluorescence monitoring at 85°C. The specificity of the amplification reaction was determined by performing a melting-curve analysis. Relative quantification of the signals was achieved by normalizing the signals of the different genes to β-actin.

Statistical analysis. All data are expressed as means ± SD. Statistical significance was evaluated by an ANOVA and a Bonferonni's adjustment applied to the results of a *t*-test with software from SPSS. A P value of <0.05 was regarded as statistically significant.

RESULTS

Cyclic strain enhances Flk-1^+ ES cell proliferation. The same number of Flk-1^+ ES cells were plated in silicon chambers; after the cells became confluent, they were subjected to cyclic strain (4, 8, or 12% strain, 1 Hz) or incubated under static conditions for 24 h. The cells were removed by trypsinization, and a Coulter counter was used to count their number (Fig. 1*A*). Cell number increased in response to cyclic strain, peaked at 8% strain, and leveled off at 12% strain. The

Table 1. *Oligonucleotide primers used for real-time PCR*

Gene	Primer Sequence	Amplified Fragment Size, bp
SM α-actin	Fwd: 5′-ACGGCCGCCTCCTCTTCCTC-3′ Rev: 5′-GCCCAGCTTCGTCGTATTCC-3′	415
SM-MHC	Fwd: 5′-GACAACTCCTCTCGCTTTGG-3′ Rev: 5′-GCTCTCCAAAAGCAGGTCAC-3′	201
SM22α	Fwd: 5′-GCAGTCCAAAATTGAGAAGA-3′ Rev: 5′-CTGTTGCTGCCCATTTGAAG-3′	507
Flk-1	Fwd: 5′-TCTGTGGTTCTGCGTGGAGA-3′ Rev: 5′-GTATCATTTCCAACCACCCT-3′	248
Flt-1	Fwd: 5′-CGGAAGCTCTGATGATGTGA-3′ Rev: 5′-TATCTTCATGGAGGCCTTGG-3′	199
VE-cadherin	Fwd: 5′-CTTCCGAATAACCAAGCAGG-3′ Rev: 5′-TACTTGACCGTGATGTTGGC-3′	369
PECAM-1	Fwd: 5′-ACATGCCATAGGCATCAGC-3′ Rev: 5′-TCACAGAGCACCGAAGTACC-3′	305
β-Actin	Fwd: 5′-GTCGTACCACAGGCATTGTGATGG-3′ Rev: 5′-GCAATGCCTGGGTGCATGGTGG-3′	493

Fwd, forward; Rev, reverse; SM, smooth muscle; MHC, myosin heavy chain; PECAM-1, platelet endothelial cell adhesion molecule-1.

increase in cell number at 8% or 12% strain was almost the same as the level induced by a maximally effective concentration of PDGF-BB (23). Flk-1$^+$ ES cells were subjected to cyclic strain (8% strain, 1 Hz) in the presence of the PDGF receptor kinase inhibitor AG-1296, which potently and selectively inhibits signaling of PDGFRα and PDGFRβ as well as of its family member *Kit* (13). AG-1296 almost completely suppressed the cyclic strain-induced increase in cell number, indicating that PDGF receptor activation is involved in the effect of cyclic strain on Flk-1$^+$ ES cell proliferation.

Flk-1$^+$ ES cells that had been cultured under static conditions or that had been exposed to cyclic strain (8%, 1 Hz) or PDGF-BB for 24 h were immunostained for an EC marker, PECAM-1, and a VSMC marker, SM α-actin (Fig. 1*B*). Under static conditions, most of the cells stained positive for SM α-actin (red) and some of the cells stained positive for PECAM-1 (green). When exposed to cyclic strain, the number of PECAM-1-positive cells decreased, whereas the number of SM α-actin-positive cells increased, and their long axis became oriented perpendicular to the direction of strain. Addition of PDGF-BB also decreased the number of PECAM-1-positive cells and increased the number of SM α-actin-positive cells, but it did not cause any change in cell orientation. The percentage of PECAM-1-positive cells determined by flow cytometry was 12.3 ± 0.25% (mean ± SD, $n = 5$) of the static control cells, 2.41 ± 0.35% of the cells exposed to cyclic strain ($P < 0.01$ vs. static control), and 3.25 ± 0.24% of the cells treated with PDGF-BB ($P < 0.01$ vs. static control).

Cyclic strain induces differentiation of Flk-1$^+$ ES cells into the VSMC lineage. Flk-1$^+$ ES cells that had been cultured under static conditions or exposed to cyclic strain (2, 4, 8, or 12%, 1 Hz) for 24 h were examined for changes in expression of various cell lineage markers. When exposed to cyclic strain, expression of the VSMC markers SM α-actin and SM-MHC increased markedly in a dose-dependent manner (Fig. 2, *A* and *B*). By contrast, cyclic strain (8%, 1 Hz, 24 h) significantly decreased the expression of the EC marker Flk-1 and had no effect on the expression of the other EC markers (Flt-1, VE-cadherin, and PECAM-1), the blood cell marker CD3, or the epithelial marker keratin (Fig. 2*C*). The addition of PDGF-BB to static Flk-1$^+$ ES cells had almost the same

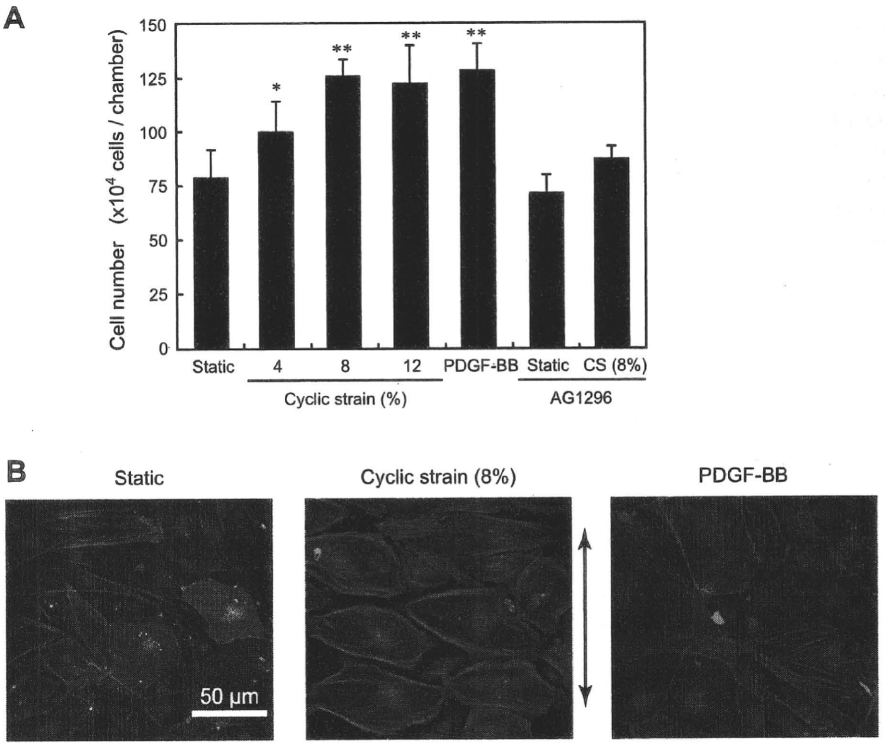

Fig. 1. Effect of cyclic strain on cell proliferation and differentiation. *A*: cell number of Flk-1-positive (Flk-1$^+$) embryonic stem (ES) cells cultured under static conditions or exposed to cyclic strain (4, 8, or 12% strain, 1 Hz) or PDGF-BB (10 ng/ml) for 24 h. Cell number increased in response to cyclic strain. The PDGF receptor β (PDGFRβ) kinase inhibitor AG-1296 (10 μmol/l) blocked the cell proliferation-promoting effect of cyclic strain. CS, cyclic strain. Values are means ± SD of data from 5 separate cell samples. *$P < 0.05$ and **$P < 0.01$ vs. static control. *B*: photomicrographs of immunostained Flk-1$^+$ ES cells cultured under static conditions or exposed to cyclic strain (8%, 1 Hz) or to PDGF-BB (10 ng/ml) for 24 h. Cells were immunostained for the endothelial cell (EC) marker platelet endothelial cell adhesion molecule 1 [PECAM-1 (green)] and a vascular smooth muscle cell (VSMC) marker [smooth muscle (SM) α-actin (red)]. The cell nuclei were stained with 4′,6-diamidino-2-phenylindole (blue). Cyclic strain and PDGF-BB increased SM α-actin-positive cells, whereas they decreased PECAM-1-positive cells. Under cyclic strain, SM α-actin-positive cells aligned themselves perpendicular to the direction of the strain. The direction of strain is from *top* to *bottom* (arrow).